LUND UNIVERSITY

On the Chemical Romance Between Gas and Surface, and how to Illuminate it

Pfaff, Sebastian

2022

Document Version:
Publisher's PDF, also known as Version of record

Link to publication

Citation for published version (APA):
Pfaff, S. (2022). *On the Chemical Romance Between Gas and Surface, and how to Illuminate it*. [Doctoral Thesis (compilation), Faculty of Engineering, LTH]. Department of Combustion Physics, Lund University.

Total number of authors:
1

General rights
Unless other specific re-use rights are stated the following general rights apply:
Copyright and moral rights for the publications made accessible in the public portal are retained by the authors and/or other copyright owners and it is a condition of accessing publications that users recognise and abide by the legal requirements associated with these rights.
• Users may download and print one copy of any publication from the public portal for the purpose of private study or research.
• You may not further distribute the material or use it for any profit-making activity or commercial gain
• You may freely distribute the URL identifying the publication in the public portal

Read more about Creative commons licenses: https://creativecommons.org/licenses/

Take down policy
If you believe that this document breaches copyright please contact us providing details, and we will remove access to the work immediately and investigate your claim.

LUND UNIVERSITY

PO Box 117
221 00 Lund
+46 46-222 00 00

Download date: 12. Oct. 2024

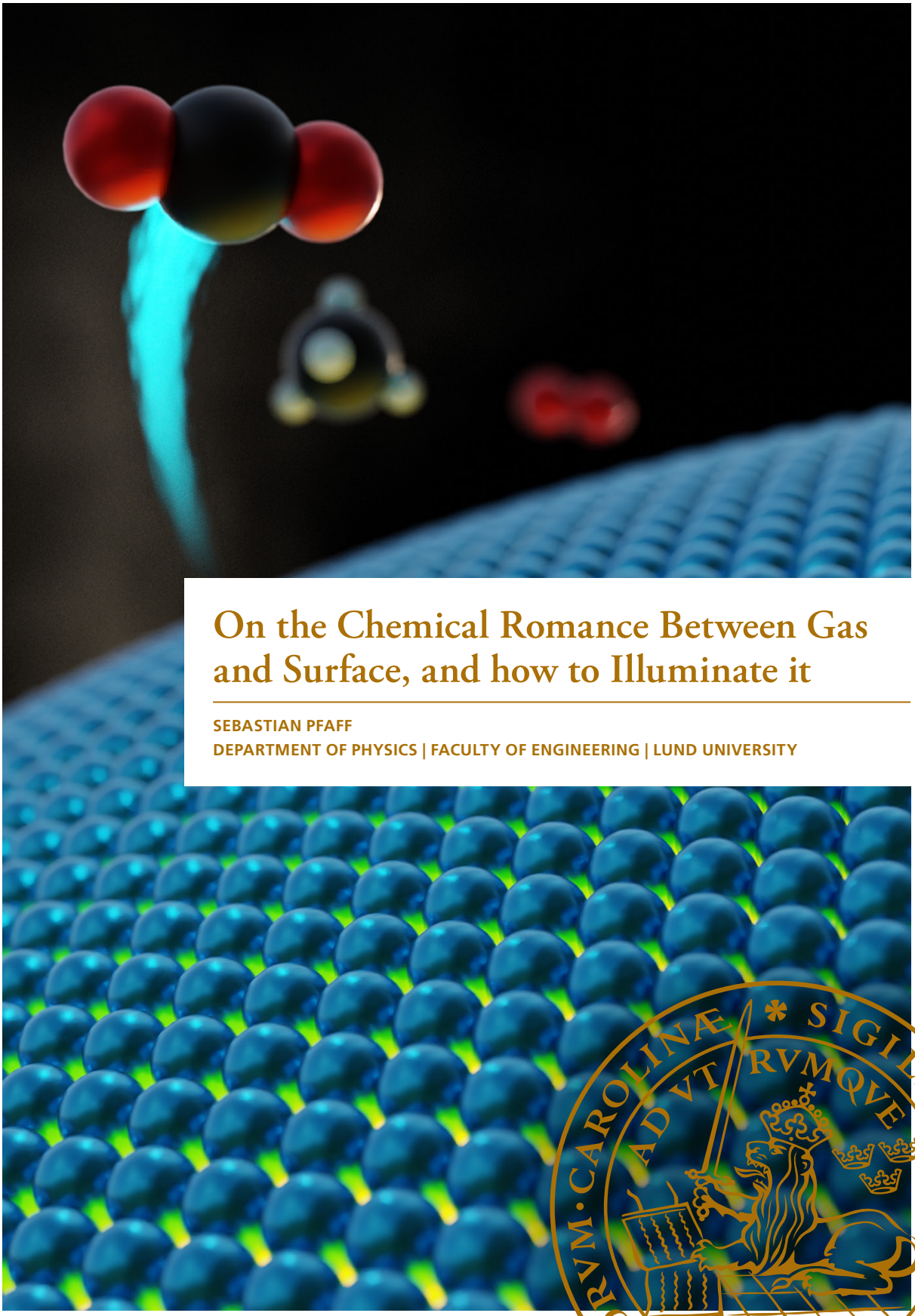

On the Chemical Romance Between Gas and Surface, and how to Illuminate it

SEBASTIAN PFAFF
DEPARTMENT OF PHYSICS | FACULTY OF ENGINEERING | LUND UNIVERSITY

On the Chemical Romance Between Gas and Surface, and how to Illuminate it

On the Chemical Romance Between Gas and Surface, and how to Illuminate it

by Sebastian Pfaff

LUND UNIVERSITY

Thesis for the degree of Doctor of Philosophy
Thesis advisors: Doc. Johan Zetterberg and Prof. Edvin Lundgren
Faculty opponent: Dr. Luca Gregoratti

To be presented, with the permission of the Faculty of Engineering at Lund University, for public criticism in the Rydberg hall at the Department of Physics on Friday, the 25th of November 2022 at 09:15.

DOKUMENTDATABLAD enl SIS 61 41 21

Organization
LUND UNIVERSITY

Department of Physics
Box 118
SE–221 00 Lund
Sweden

Document name
DOCTORAL DISSERTATION

Date of disputation
2022-11-25

Sponsoring organization

Author(s)
Sebastian Pfaff

Title and subtitle
On the Chemical Romance Between Gas and Surface, and how to Illuminate it

Abstract
An increasing number of catalysis experiments are conducted at higher pressures to bridge the pressure gap. This means that we need to measure not only the sample surface but also the gas phase around the sample with spatial resolution. This thesis treats the development and applications of two optical techniques that can be used to image the surface of a model catalyst together with the surrounding gas: planar laser-induced fluorescence (PLIF) and 2D-surface optical reflectance (2D-SOR). The strengths and weaknesses of the techniques are discussed. Examples are used to show how the techniques can be applied to study active model catalysts *in situ* under ambient pressure conditions.

PLIF is used to image the CO and CO_2 concentrations around various Pd model catalysts during the CO oxidation reaction. 2D-SOR is used to show the surface oxidation process during the same reaction. We show how PLIF and 2D-SOR can be combined with additional techniques, primarily high-energy surface X-ray diffraction (HESXRD), thermography, mass spectrometry (MS) and polarisation modulation infrared reflection absorption spectroscopy (PMIRRAS).

Finally, we show how PLIF and 2D-SOR can be used to bridge the so-called materials gap by taking advantage of the spatial resolution of the techniques to study polycrystalline samples. These samples, which exhibit a plethora of surface structures, can be seen as a step towards more industry-like samples.

Key words
planar laser-induced fluorescence, surface optical reflectance, model catalysis, palladium, polycrystal, CO oxidation, heterogeneous catalysis

Classification system and/or index terms (if any)

Supplementary bibliographical information

Language
English

ISSN and key title

ISBN
978-91-8039-424-6 (print)
978-91-8039-423-9 (pdf)

Recipient's notes

Number of pages
197

Price

Security classification

I, the undersigned, being the copyright owner of the abstract of the above-mentioned dissertation, hereby grant to all reference sources the permission to publish and disseminate the abstract of the above-mentioned dissertation.

Signature _____ Date 2022-10-17

On the Chemical Romance Between Gas and Surface, and how to Illuminate it

by Sebastian Pfaff

LUND UNIVERSITY

Cover illustration front: A metal surface interacting with gas molecules.

Cover illustration back: The oxide thickness on palladium as function of the step density parameter. See Chapter 6.

Funding information: The thesis work was financially supported by the Swedish Research Council (project no. 2016-03501), the Swedish Foundation for Strategic Research (project no. ITM17-0045), the Åforsk Foundation and the Crafoord Foundation.

pp. 1–71 © Sebastian Pfaff 2022
Papers I, II, III, IV, V, VII, VIII and IX © The Authors
Paper VI © 2019 IOP Publishing

Faculty of Engineering, Department of Physics

ISBN: 978-91-8039-424-6 (print)
ISBN: 978-91-8039-423-9 (pdf)
LRCP: LRCP-244
ISSN: 1102-8718
ISRN: LUTFD2/TFCP-244-SE

Typeset 17th October 2022 with XƎLaTeX.
Printed in Sweden by Media-Tryck, Lund University, Lund 2022

Dedicated to all the amazing people who I have met in my 11 years as a student at Lund University.

Contents

List of publications iv
Related Work v
Abstract vi
Popular Summary in English vii
Populärwissenschaftliche Zusammenfassung auf Deutsch ix
Populärvetenskaplig sammanfattning på svenska xi
Acknowledgements xiii

1 Introduction **1**

2 Surface Crystallography **5**
2.1 Adsorption of Gases 8

3 The Gaps to Industry **9**
3.1 The Materials Gap 10
3.1.1 Single Crystals 11
3.1.2 Curved Crystals 12
3.1.3 Polycrystals 13
3.2 The Pressure Gap 15
3.2.1 Pressure Matters 16
3.2.2 Gas Diffusion 17
3.2.3 Gas Temperature 18
3.3 The Reactor Gap 18

4 Catalysis and CO Oxidation over Pd(100) **21**
4.1 Why Pd and the Volcano Plot 21
4.2 The Arrhenius Equation and CO Oxidation 22
4.2.1 The Catalytic Ignition 23

5 Techniques and Equipment **25**
5.1 Reactor and Gas System 25
5.2 Laser Systems and Detectors 28
5.3 Planar Laser Induced Fluorescence PLIF 28
5.3.1 CO_2 Detection 29
5.3.2 CO Detection 31

5.3.3 Data Analysis . . . 31
5.3.4 Quenching . . . 35
5.3.5 The Choice of Colour Map . . . 37
5.3.6 This Thesis . . . 38
5.4 Temperature Measurements . . . 38
5.4.1 Sample Temperature . . . 39
5.4.2 Gas Temperature . . . 39
5.5 2D-Surface Optical Reflectance Microscopy 2D-SOR . . . 40
5.5.1 Theory . . . 41
5.5.2 Data Evaluation . . . 44
5.5.3 Conclusions . . . 45
5.6 Other Techniques Combined with 2D-SOR or PLIF . . . 46
5.6.1 High-Energy Surface X-Ray Diffraction HESXRD . . . 46
5.6.2 Electron Backscatter Diffraction EBSD . . . 46
5.6.3 Polarisation Modulation Infrared Reflection Absorption Spectroscopy PMIRRAS . . . 47
5.7 Combining Techniques . . . 47

6 Experimental Highlights **51**
6.1 Reaction Oscillations during CO Oxidation . . . 51
6.2 Visualizing the Ignition of Pd(100) Single Crystal . . . 54
6.3 Polycrystal Ignition . . . 55
6.4 Polycrystals with Small Grains . . . 56

7 Outlook **61**
References . . . 63

8 Scientific Publications **69**
8.1 Author Contributions . . . 69
Paper I: A Convenient Setup for Laser-Induced Fluorescence Imaging of both CO and CO_2 during Catalytic CO Oxidation . . . 73
Paper II: Combining Synchrotron Light with Laser Technology in Catalysis Research . . . 83
Paper III: Combining High-Energy X-Ray Diffraction with Surface Optical Reflectance and Planar Laser Induced Fluorescence for *Operando* Catalyst Surface Characterization . . . 91
Paper IV: Surface Optical Reflectance combined with X-Ray Techniques during Gas-Surface Interactions . . . 103
Paper V: Combining Planar Laser-Induced Fluorescence with Stagnation Point Flows for Small Single-Crystal Model Catalysts: CO Oxidation on a Pd(100) 115
Paper VI: Temperature Characterization of an *Operando* Flow Reactor for Heterogeneous Catalysis . . . 129

Paper VII: Infrared Surface Spectroscopy and Surface Optical Reflectance for *Operando* Catalyst Surface Characterization 143
Paper VIII: *Operando* Reflectance Microscopy on Polycrystalline Surfaces in Thermal Catalysis, Electrocatalysis, and Corrosion 153
Paper IX: Visualizing the Gas Diffusion Induced Ignition of a Catalytic Reaction 167

List of publications

This thesis is based on the following publications, referred to by their Roman numerals.

I. Zhou, J., Pfaff, S., Lundgren, E. & Zetterberg, J. **A Convenient Setup for Laser-Induced Fluorescence Imaging of both CO and CO_2 during Catalytic CO Oxidation**. *Applied Physics B* **123,** 87 (2017).

II. Blomberg, S., Zetterberg, J., Gustafson, J., Zhou, J., Shipilin, M., Pfaff, S., Hejral, U., Carlsson, P.-A., Gutowski, O., Bertram, F. & Lundgren, E. **Combining Synchrotron Light with Laser Technology in Catalysis Research**. *Journal of Synchrotron Radiation* **25,** 1389–1394 (2018).

III. Pfaff, S., Zhou, J., Hejral, U., Gustafson, J., Shipilin, M., Albertin, S., Blomberg, S., Gutowski, O., Dippel, A., Lundgren, E. & Zetterberg, J. **Combining High-Energy X-Ray Diffraction with Surface Optical Reflectance and Planar Laser Induced Fluorescence for *Operando* Catalyst Surface Characterization**. *Review of Scientific Instruments* **90,** 033703 (Mar. 2019).

IV. Albertin, S., Gustafson, J., Zhou, J., Pfaff, S., Shipilin, M., Blomberg, S., Merte, L. R., Gutowski, O., Dippel, A. C., Zetterberg, J., Lundgren, E. & Hejral, U. **Surface Optical Reflectance combined with X-Ray Techniques during Gas-Surface Interactions**. *Journal of Physics D: Applied Physics* **53,** 224001 (Apr. 2020).

V. Zhou, J., Matera, S., Pfaff, S., Blomberg, S., Lundgren, E. & Zetterberg, J. **Combining Planar Laser-Induced Fluorescence with Stagnation Point Flows for Small Single-Crystal Model Catalysts: CO Oxidation on a Pd(100)**. *Catalysts 2019, Vol. 9, Page 484* **9,** 484 (May 2019).

VI. Pfaff, S., Karlsson, H., Nada, F. A., Lundgren, E. & Zetterberg, J. **Temperature Characterization of an *Operando* Flow Reactor for Heterogeneous Catalysis**. *Journal of Physics D: Applied Physics* **52,** 324003 (Aug. 2019).

VII. Rämisch, L., Gericke, S. M., Pfaff, S., Lundgren, E. & Zetterberg, J. **Infrared Surface Spectroscopy and Surface Optical Reflectance for *Operando* Catalyst Surface Characterization**. *Applied Surface Science* **578,** 152048 (Mar. 2022).

VIII. Pfaff, S., Larsson, A., Orlov, D., Harlow, G. S., Abbondanza, G., Linpé, W., Rämisch, L., Gericke, S. M., Zetterberg, J. & Lundgren, E. ***Operando* Reflectance Microscopy on Polycrystalline Surfaces in Thermal Catalysis, Electrocatalysis, and Corrosion**. *ACS Applied Materials & Interfaces* **13,** 19530–19540 (Apr. 2021).

IX. Pfaff, S., Rämisch, L., Gericke, S. M., Larsson, A., Lundgren, E. & Zetterberg, J. **Visualizing the Gas Diffusion Induced Ignition of a Catalytic Reaction**. *ACS Catalysis* (2022).

Related Work

The following papers are related work, and are referred to with capital letters. They mainly concern applications of 2D-SOR in electrochemistry and cases where I have performed measurements with optical techniques developed by me.

A. Garcia-Martinez, F., García-Fernández, C., Simonovis, J. P., Hunt, A., Walter, A., Waluyo, I., Bertram, F., Merte, L. R., Shipilin, M., Pfaff, S., Blomberg, S., Zetterberg, J., Gustafson, J., Lundgren, E., Sánchez-Portal, D., Schiller, F. & Ortega, J. E. **Catalytic Oxidation of CO on a Curved Pt(111) Surface: Simultaneous Ignition at All Facets through a Transient CO-O Complex**. *Angewandte Chemie International Edition* **59,** 20037–20043 (Nov. 2020).

B. Linpé, W., Harlow, G. S., Larsson, A., Abbondanza, G., Rämisch, L., Pfaff, S., Zetterberg, J., Evertsson, J. & Lundgren, E. **An electrochemical cell for 2-dimensional surface optical reflectance during anodization and cyclic voltammetry**. *Review of Scientific Instruments* **91,** 044101 (Apr. 2020).

C. Linpé, W., Rämisch, L., Abbondanza, G., Larsson, A., Pfaff, S., Jacobse, L., Zetterberg, J., Merte, L., Stierle, A., Hegedues, Z., Lienert, U., Lundgren, E. & Harlow, G. S. **Revisiting Optical Reflectance from Au(111) Electrode Surfaces with Combined High-Energy Surface X-ray Diffraction**. *Journal of The Electrochemical Society* **168,** 096511 (Sept. 2021).

D. Bao, Y., Dorozynska, K., Stamatoglou, P., Kong, C., Hurtig, T., Pfaff, S., Zetterberg, J., Richter, M., Kristensson, E. & Ehn, A. **Single-shot 3D imaging of hydroxyl radicals in the vicinity of a gliding arc discharge**. *Plasma Sources Science and Technology* **30,** 04LT04 (Apr. 2021).

E. García-Martínez, F., Rämisch, L., Ali, K., Waluyo, I., Bodero, R. C., Pfaff, S., Villar-García, I. J., Walter, A. L., Hunt, A., Pérez-Dieste, V., Zetterberg, J., Lundgren, E., Schiller, F. & Ortega, J. E. **Structure Matters: Asymmetric CO Oxidation at Rh Steps with Different Atomic Packing**. *Journal of the American Chemical Society* **2022,** 15363–15371 (2022).

All papers are reproduced with permission of their respective publishers.

Abstract

An increasing number of catalysis experiments are conducted at higher pressures to bridge the pressure gap. This means that we need to measure not only the sample surface but also the gas phase around the sample with spatial resolution. This thesis treats the development and applications of two optical techniques that can be used to image the surface of a model catalyst together with the surrounding gas: planar laser-induced fluorescence (PLIF) and 2D-surface optical reflectance (2D-SOR). The strengths and weaknesses of the techniques are discussed. Examples are used to show how the techniques can be applied to study active model catalysts *in situ* under ambient pressure conditions.

PLIF is used to image the CO and CO_2 concentrations around various Pd model catalysts during the CO oxidation reaction. 2D-SOR is used to show the surface oxidation process during the same reaction. We show how PLIF and 2D-SOR can be combined with additional techniques, primarily high-energy surface X-ray diffraction (HESXRD), thermography, mass spectrometry (MS) and polarisation modulation infrared reflection absorption spectroscopy (PMIRRAS).

Finally, we show how PLIF and 2D-SOR can be used to bridge the so-called materials gap by taking advantage of the spatial resolution of the techniques to study polycrystalline samples. These samples, which exhibit a plethora of surface structures, can be seen as a step towards more industry-like samples.

Popular Summary in English

As perhaps hinted at by the title, this thesis is about developing optical techniques to better understand catalytic chemical reactions between gases and (metal) surfaces. So what does that mean and why is it important, you might ask? Catalysis is the concept of making a chemical reaction take a different reaction pathway by means of adding a compound — a catalyst — to the reaction. The catalyst takes part in the reaction but then, importantly, returns to its original state so it can be a part of yet another reaction cycle. The new reaction pathway may then result in fewer waste products being created or that less pressure or heat are needed for the reaction to work.

Now, for some readers, the word catalysis brings the mind to a set of rather expensive automotive components that are often stolen for their valuable precious metals. At least while we are still in the combustion-engine era. The reason why we use these precious metals is that they are reactive enough for gases to attach to them, but not so reactive that the reactants or any new molecules that might be created by the chemical reaction do not detach, which would mean that the catalyst could not return to its original state. In Swedish terms, these metals are *lagom* reactive, just reactive enough. The fact that many catalysts used today are very expensive and also scarce on the Earth is, of course, also an issue, both due to environmental and humanitarian concerns when mining these metals and due to their price, which makes it difficult and expensive to use these catalysts at a large scale.

Thus, it would be useful to be able to design new catalysts on the basis of our knowledge of how the existing ones work. Perhaps we could design those that are much more efficient, exhibit a better selectivity towards a certain end product, or perhaps we can use cheaper materials. To do this, we need to have a full understanding of what is going on at the surface of the catalysts that we use today. Where do the gas molecules attach to the surface, will the surface oxidise, and how does that affect the reaction? Do the gas molecules move around on the surface before they react, do they maybe move to a step or a kink in the metal surface? In a way, we would like to know the role of every surface feature and whether it has an impact on the catalytic process.

Now we finally return to what this thesis is about, the development and deployment of new optical techniques that can be used to see what is going on at the catalyst surface and also in the gas surrounding the catalyst. Focus lies on the further development and applications of two techniques in particular, Planar Laser Induced Flourescense (PLIF) and 2D Surface Optical Reflectance (2D-SOR). In PLIF, a laser is used to excite one of the gases involved in the catalytic reaction, causing it to emit light. This light can then be photographed with a camera, telling us where in space the gas is. In contrast, SOR tells us information about the catalyst surface by taking pictures of the sample surface illuminated with LED light. From this we can see whether the chemical environment changes at each point on the surface.

The thesis also treats how to combine the aforementioned techniques and what can be learned from the combination, à la the 1+1=3 slogan known from the marketing industry. For example, it turns out that the gas surrounding the catalyst has a large impact on the sample surface, which would have been difficult to determine without combining gas and surface sensitive techniques. The purpose of all new methods described in this thesis is to in the end find out more details on what is going on at the surface of the catalysts. Eventually, the new knowledge can be used in the quest to develop more efficient catalysts.

Populärwissenschaftliche Zusammenfassung auf Deutsch

Wie der Titel schon erwarten lässt, beschreibt diese Doktorarbeit die Entwicklung optischer Messtechniken, die es erlauben, katalytische chemische Reaktionen zwischen Gasen und (Metall-) Oberflächen besser zu verstehen. Was bedeutet das also und warum ist es wichtig, fragen Sie sich vielleicht? Katalyse ist das Konzept, eine chemische Reaktion zu beeinflussen, indem ein neuer Stoff – der Katalysator – hinzugefügt wird, der an der Reaktion teilnimmt. Der Katalysator wird aber – und das ist wichtig – unverändert wieder freigesetzt, kann daher wiederum Teil einer weiteren Reaktion sein und viele solcher Katalysezyklen durchlaufen. Katalyse kann dann dazu führen, dass weniger Abfallprodukte erzeugt werden oder dass für die Reaktion weniger Druck oder Wärme benötigt werden.

Viele Leser werden bei dem Wort Katalyse an eine Reihe teurer Automobilkomponenten denken, die oft wegen der in ihnen enthaltenen wertvollen Edelmetalle gestohlen werden (zumindest solange wir uns noch im Zeitalter der Verbrennungsmotoren befinden). Diese Edelmetalle werden verwendet, weil sie reaktiv genug sind, damit sich Gase an sie anlagern können, aber nicht so reaktiv, dass sich die Reaktanten oder neue Moleküle, die durch die chemische Reaktion entstehen könnten, nicht mehr lösen. Wenn dies der Fall wäre, könnte der Katalysator nicht in den ursprünglichen Zustand zurückkehren. Im Schwedischen gibt es dafür den Begriff „lagom“ – gerade richtig: Katalysatoren sind „lagom“ reaktiv, gerade reaktiv genug, und nicht zu reaktiv.

Dass viele heute verwendete Katalysatoren sehr teuer und auf der Erde auch knapp sind, ist ein Problem, einerseits weil es ökologische und humanitäre Bedenken in Bezug auf den Abbau dieser Metalle gibt, andererseits weil ihr hoher Preise den Einsatz dieser Katalysatoren im großen Maßstab erschwert und verteuert.

Daher wäre es nützlich, unser Wissens über die Funktionsweise dieser Katalysatoren zu nutzen um neue Katalysatoren entwickeln, die effizienter sind, eine bessere Selektivität für ein bestimmtes Endprodukt aufweisen, oder aus billigeren Materialien hergestellt können. Dazu müssen wir verstehen, was an der Oberfläche der Katalysatoren vor sich geht, die wir heute verwenden. Wo genau an der Oberfläche lagern sich die Gasmoleküle ab, oxidiert die Oberfläche und wie wirkt sich das auf die Reaktion aus? Bewegen sich die Gasmoleküle auf der Oberfläche, bevor sie reagieren, bewegen sie sich vielleicht zu einer Stufe im Gitter des Metalls, oder einem Knick in der Metalloberfläche? In gewisser Weise möchten wir wissen, welche Rolle jedes Oberflächenmerkmal hat und ob es einen Einfluss auf den Prozess der Katalyse hat.

Und damit kommen wir endlich zum Inhalt dieser Arbeit, der Entwicklung und dem Einsatz neuer Messtechniken, die verwendet werden können, um die Vorgänge an der Katalysatoroberfläche und in dem den Katalysator umgebenden Gas zu verstehen. Der Fokus liegt dabei auf der Weiterentwicklung und Anwendung von insbesondere zwei Techniken,

planare laserinduzierte Fluoreszenz (Planar Laser Induced Flourescense – PLIF) und Optische Oberflächenreflexion (Surface Optical Reflectance – SOR). Bei PLIF wird ein Laser verwendet, um eines der an der katalytischen Reaktion beteiligten Gase zum Leuchten anzuregen. Das Leuchten kann mit einer Kamera fotografiert werden und Aufschluss darüber geben, wo sich wie viel Gas befindet. Die zweidimensionale (2D) SOR gibt uns dagegen Information über die Oberfläche des Katalysators. Dazu erstellt die Technik Bilder von der mit LED-Licht beleuchteten Oberfläche. Aus den Bildern können wir erkennen, ob sich die chemische Umgebung an jedem Punkt der Oberfläche ändert.

Diese Doktorarbeit befasst sich auch damit, was wir durch die Kombination dieser beiden Methoden zusätzlich lernen können, gemäss des Prinzips „das Ganze ist mehr als die Summe seiner Teile“ oder des aus dem Marketing bekannten Slogans „1+1=3 “. Beispielsweise hat sich herausgestellt, dass das Gas, welches den Katalysator umgibt, einen großen Einfluss auf die Probenoberfläche hat, was ohne die Kombination von gas- und oberflächenempfindlichen Techniken schwer zu bestimmen gewesen wäre. All die neuen Methoden, die hier beschrieben werden, dienen dazu herauszufinden, was an den Katalysatoroberflächen im Detail vor sich geht, und im Endeffekt können die so gewonnenen Erkenntnisse zur Entwicklung von effizienteren Katalysatoren führen.

Populärvetenskaplig sammanfattning på svenska

Som titeln antyder handlar denna avhandling om utveckling av optiska mättekniker som hjälper oss att förstå katalytiska kemiska reaktioner mellan gaser och metallytor. Så vad är katalys och varför är det viktigt? Katalys är konceptet att få en kemisk reaktion att ta en alternativ väg med en annan reaktionsmekanism genom att lägga till ett ämne — katalysatorn — till reaktionen. Detta ämne blir inblandat i reaktionen, men ska efter att reaktionen är avslutad återigen vara i sitt originaltillstånd så att det kan bli del av ytterligare en reaktion. Om och om igen. Den nya reaktionsvägen kan då innebära exempelvis att mindre energi behövs för reaktionen eller att det skapas färre miljöfarliga biprodukter.

För många väcker nog ordet katalys tankar av en rätt dyr bildel som inte sällan blir stulen, i alla fall nu medan vi fortfarande använder bilar med förbränningsmotorer (hej du som läser detta i 2040 och inte kan relatera). Det är självklart inte bildelen som sådan tjuvarna är ute efter, utan snarare de dyra metallerna som är den aktiva komponenten i en bilkatalysator. Anledningen till att vi använder dessa dyra metaller är att de är tillräckligt reaktiva för att gaser ska fastna på metallytan och interagera med den, men inte så reaktiva att produkterna som skapas i reaktioner på metallytan aldrig lossnar. Den sista biten är väldigt viktig, för om reaktionsprodukterna aldrig lossnar blockeras metallytan och blir då otillgänglig för framtida reaktioner. Ytan ska alltså vara lagom reaktiv. Många av dessa lagom reaktiva grundämnen, som idag används i som katalysatorer är väldigt dyra, eftersom de är rätt sällsynta i jordskorpan och dyra att bryta och utvinna. Därtill kommer humanitära- och miljöaspekter vid brytning av dessa grundämnen som inte sällan sker i konfliktområden.

Det är därför av intresse att ta fram nya typer av katalysatorer, baserat på den kunskap vi har i nuläget. Det går kanske att designa katalysatorer som fungerar vid lägre temperaturer eller tryck, eller sådana som består av billigare och mindre problematiska grundämnen. För att kunna göra detta behöver vi få svar på en del frågor kring de kemiska reaktionerna. Vad sker på ytan av katalysatormaterialen? Var på metallytan fastnar gasmolekylerna och var sker själva reaktionen? Flyttar sig gasmolekylerna på ytan så att de fastnar på ett ställe men reagerar på ett annat? Rör de sig till steg eller andra ojämnheter i ytstrukturen? Vi vill ta reda på vilken roll alla delar av ytan spelar för den katalytiska processen.

Nu återkommer vi äntligen till vad denna avhandlingen handlar om, nämligen utvecklingen av nya optiska mätteknikter som hjälper oss att bättre förstå både vad som händer på ytan av en katalysator och i gasblandningen precis ovanför ytan. Fokus har legat på utvecklingen och tillämpningen av två tekniker: laserinducerad fluorescens i planet (Planar Laser Induced Flourescense), förkortat PLIF och optisk ytreflektion (Surface Optical Reflectance), förkortat SOR. PLIF innebär att en laserstråle av en specifik färg används för att få en av de inblandade gaserna att lysa genom fluorescens. När gasen väl lyser kan man ta en bild på den lysande gasen med en kamera. På så sätt kan man mäta var gasen finns samt

hur mycket gas det är på olika ställen. Vid SOR används en vanlig röd LED-lampa för att lysa på en katalysatormetallbit. Ljuset får studsa på metallbiten som beter sig lite som en badrumsspegel. Om metallbiten har blivit oxiderad eller ojämn av den kemiska reaktionen reflekterar den sämre. Genom att titta på reflektionen från LED-lampan på metallbiten i ett mikroskop kan man se var på metallbiten det har bildats oxider.

Denna avhandling tar också upp hur det går att kombinera de nämnda teknikerna med ytterligare tekniker för att få ut ännu mer av en och samma mätning. Vid en sådan kombinerad mätning visade det sig till exempel att gasen vid ytan har en stor påverkan på ytans struktur, något som hade varit svårt att se annars. Sammanfattningsvis är syftet med all denna teknikutveckling att bättre kunna förstå vad som händer vid ytan av katalysatorerna; en förståelse som sedan kan leda till utvecklingen av mer effektiva katalysatorer.

Acknowledgements

We are told when writing papers that the only parts to which people really pay attention are the abstract and figures, not because the rest is not interesting, but because the abstract and figures should contain everything that is really important. In a thesis, in my experience, there is only one such important part, and you are reading it right now. So if this is the first page you opened, no shame on you. If not, then wow, apparently the research I have done the past five years is also interesting.

I naturally begin the actual list of people with my supervisor **Johan Zetterberg**. You have really helped me develop as a researcher and also as a person over the many years we have known each other. You have tirelessly read my manuscripts, given advice, and always been available for a short discussion or a longer rant. Also, you gave me the possibility to travel to many conferences all over the world, something that I know that I should not take for granted and am very grateful for. Finally, you placed a lot of trust in me by choosing to have me as your student. I am very grateful for that trust.

Next comes my co-supervisor **Edvin Lundgren**. Your office door have always been open for a quick (or not so quick) chat, and you always had time to listen to me when I had questions or concerns. Your great sense of humor also made the many beam times and conferences you joined us on very enjoyable, and let's not forget that you were the one always making sure us student got enough to eat while measuring. I am also constantly impressed by your ability to seemingly memorize an infinite amount of literature. You always knew which paper to read on basically anything surface science related.

None of the paper writing would be possible had I not gotten the best introduction to the lab work I could think of. **Jianfeng Zhou**, you supervised me during my bachelors and masters theses, taught me much of what I know about lasers, while also guiding me to become a good scientist. I do miss hanging out with you and our lunches at Finn Inn. Thank you so much for everything.

Soon Jianfeng left, I got two new amazing colleagues, **Sabrina Gericke** and **Lisa Rämisch**, you are both amazingly smart, and have made everything we have done together, whether it is beamtimes or long lab nights, a breeze. Sabrina, thank you for all the help I got from you when working with XPS spectra, and thank you for all the sometimes very deep discussions on academia, life and whatnot during our many night shifts together at beamtimes. Lisa, thank you for sharing your hype and energy about anything laser or measurement related, it has been amazing. Also, thank you for hyping me and the rest of us to go for pub nights, Lillsjödal and other fun activities.

Alfred Larsson, we have spent countless hours together in the lab during late-night measurements resulting, having a good time while producing amazing data. On top of that, you

were always down for a nice trip. Oh, and I still remember when you called me all excited about that idea of plotting the 2D-SOR data in the stereographic triangle.

During this PhD, I have been on countless beamtimes and collaborations, which have been enjoyable mainly because the very nice people with whom I got to share them. **Uta Hejral**, **Stefano Albertin**, **Johan Gustafson**, **Weronica Linpé**, **Giuseppe Abbondanza**, **Volkmar Koller**, **Marcel Abb**, **Dorotea Gajdek**, **Harald Wallander**, thank you for making the many beam times enjoyable. **Gary Harlow**, thank you for teaching me so much about HESXRD and software development. Sorry for the messy HAT code that you had to... ahem... rewrite. **Fernando García Martínez**, thank you for some nice nights measuring the curved crystals, we got some very nice results from that. Special thanks also goes to **Sara Blomberg**. Except for the night shifts at beam times we have spent together, you gave me lots of advice on the thesis writing process. **Dmitry Orlow**, thank you for taking the time to thoroughly explain the quirks of metallurgy and the details regarding the EBSD data. **Christoffer Pichler**, thanks for starting to develop our baby, the LabView software.

I also have to thank the Bachelor students who I supervised during their thesis projects. You were all incredibly fun and inspiring to work with. **Philip Stjärneblad**, you tirelessly performed quenching measurements, the results of which are actually featured in this thesis. **Luuk Kempen**, you kept finding new ways to optimise PLIF data analysis and taught me some Python quirks that I was not aware of. **Hanna Sjö**, you did an amazing job analysing extremely messy PLIF data, and now it seems that you may be on your way into the same rabbit hole that I fell into concerning polycrystals.

Of course, I also owe a lot to those people who have ensured that the atmosphere at the division remains friendly, cosy, and a place I want do go to (almost) every day. **Haisol Kim**, thanks for being a great office mate and for helping me procrastinate for hours with long and wonderful discussions about life, love, how to not procrastinate, and everything in between. **Per-Erik Bengtsson**, you made sure to let us know that you were always there for us and that we could always talk to you should we have any problems. Thank you very much for that. **Minna Ramkull**, **Emelie Niléhn** and **Cecilia Bille**, thank you for solving all the problems with Ladok, money, the coffee machine, registrations, and much more which I probably have not even noticed because you solved them before they became actual problems. **Igor Buzuk**, thank you for tirelessly reinstalling Windows for me on countless computers and reminding me when the IT security of our group was not up to par, which happened quite often, to be frank. A very large thank you should also be directed to **Trivselgruppen**, for all the fun activities that you hosted over the years. Big thanks also go **Pernilla Helmer** for proofreading the popular science abstract.

Finally, I also would like to thank all volunteers at the student unions, primarily those at TLTH, LDK, Dokt and LUS, but also those involved in SFS and SFS-DK, for always fighting for the rights of us doctoral students. Thank you for all the hard work.

Chapter 1

Introduction

Chemical reactions are the cornerstone of any life on Earth, and many of these use some kind of catalyst. A catalyst is a compound — let us stay generic for now — that increases the rate of these reactions[1]. In living things, these compounds are called enzymes; one example is the chlorophyll in plants that enables plants to convert energy and CO_2 into hydrocarbons. Another example from our bodies is lactase, which ensures that we can digest milk properly. In the chemical industry, catalysts are involved in the production of most chemicals. In fact, if it were not for the Haber-Bosch process, one of the most famous catalytic processes whereby nitrogen from the atmosphere is bound to produce fertiliser, much of the world's population would probably not be alive today[2].

In industrial catalysis, one separates between homogeneous catalysis and heterogeneous catalysis. In the first case, the catalyst is in the same phase as the reactants, often in the liquid phase. In the latter case, the catalyst is in a phase different from that of the reactants and products. Here, the catalyst is often a solid metal or metal oxide while the reactants are delivered in liquid or gas phase. The reaction then takes place at the interface between the solid and the gas or liquid. This thesis will focus on heterogeneous catalysis. Because catalysis is so prevalent in industry, there is great interest in developing novel, less expensive catalysts that exhibit larger selectivity toward the desired end-product. This means that the process produces fewer by-products. In addition, there is interest in performing the reactions at lower temperatures and pressures to lower the energy consumption and reactor complexity.

In order to develop new catalysts, we first have to understand the chemical reactions that take place at the surfaces of the catalytically active nanoparticles commonly used in industry, preferably as detailed as possible. This means all the way to the "that atom binds here, this atom creates bond with this other atom, and that atom detaches from here" level.

Naturally, nanoparticles are quite complicated to study, especially in a chemical environment where there is a constant interaction with the surrounding medium. They are small, all over the place, and their individual surfaces are so small that it is difficult to obtain any surface structure information. Thus, one uses so-called model catalysts that are flat and have a well-defined surface. One can then relate the activity with the surface structure and one can also take advantage of simulations to further understand what is happening at the surface[2]. However, this presents an issue in that, in the process of making the experiments possible, one must simplify the shape or form of the catalyst, which means the results found may or may not apply to industry. This is called the *material gap*.

In order to study the surface, one must somehow probe it and record some response to the probe. It turns out that electrons are a great probe for anything surface-related, as they can travel only a very short distance in a solid. Thus, any time electrons are used as probes or when electrons are emitted as a result of the experiment, one can be quite sure that the majority of the signal originates from the sample surface and not the bulk. The issue with electron-based techniques is that in their primitive form they do not work if the sample is surrounded by higher pressure gas, as is common when catalysts are used in industry; the aforementioned Haber-Bosch process, for instance, is performed at pressures of around 300 bar, several orders of magnitude from the 10^{-6} mbar at which electrons can be easily used. The result of this is that many studies are performed in the low-pressure regime with little concern for how the surface is affected by being exposed to high-pressure gases. This is called the *pressure gap*.

Of course, there is interest in bridging these gaps by developing experimental techniques that can be used during catalysis experiments at high pressures and on samples that are as close to those used in industry as possible. Therefore, much effort has been put into developing these so-called *operando* capable techniques, which can probe the active catalyst sample under industry-like conditions[3, 4]. Examples of such techniques are Ambient Pressure X-Ray Photoelectron Spectroscopy (AP-XPS)[5, 6], High-Energy Surface X-Ray Diffraction (HESXRD)[7], or High Pressure Scanning Tunnelling Microscopy[8].

Although these techniques work under higher pressures, none of them provide spatial resolution over a larger area. In addition, the techniques primarily provide information on the sample surface. While APXPS does provide some information on major species in the gas phase, it only provides surface and gas phase data from a very localised area. To remedy this, development has been made on optical techniques that can be used to augment the aforementioned set of techniques. Optical techniques are well-suited for this, as light is normally able to penetrate gas, even if the gas is at high pressures. Planar Laser-Induced Fluorescence (PLIF), a technique commonly used to study the gas phase in combustion and flame diagnostics, has been adapted to work in catalysis applications[9, 10]. In addition to this, 2D-Surface Optical Reflectance (2D-SOR) was developed as a simple and inexpensive technique to probe the sample surface with spatial resolution[11–13].

In this work, the PLIF and 2D-SOR techniques have been further developed and combined with synchrotron-based techniques in *operando* studies to bridge the aforementioned pressure and material gaps. The techniques are demonstrated primarily by studying the oxidation of CO to CO_2 using Pd catalysts, a commonly studied model system[14]. Paper I discusses the development of a rather compact PLIF system to detect CO and CO_2, which can be brought to synchrotrons to be combined with other techniques. Papers II and III demonstrate the use of this setup at DESY, where we combine the PLIF and 2D-SOR techniques with HESXRD to study catalytic oscillations on Pd(100). We have also used HESXRD to study how the 2D-SOR signal correlates with the formation of surface oxides, which is demonstrated in Paper IV. 2D-SOR was also correlated with PM-IRRAS, as demonstrated in Paper VII. To better understand how pressure affects gas diffusion and gas temperature, these effects have also been studied, as discussed in Papers V and VI, respectively. Paper IX shows, with a combination of PLIF, 2D-SOR and thermography, that the gas diffusion even is the driving force of the catalytic ignition of highly active model catalysts at higher pressures.

To bridge the material gap, 2D-SOR has been used to study polycrystalline samples, where each grain is treated as a single crystal surface. This enables the study of many surface orientations at once, further closing the gap to industry as demonstrated in Paper VIII.

In addition to what is shown in the papers, much work within the scope of this thesis has gone towards improving the experimental setup and the data management. In particular, the PLIF setup has been improved to allow for simultaneous thermography and PLIF measurements. The software to control the experiments has been continuously worked on to further automate data acquisition, resulting in more repeatable measurements. Significant effort was also spent on the data analysis of the 2D-SOR data of polycrystals, by directly relating it to the surface orientation data, which enables the plotting of these data in the so-called stereographic triangle. More on this in Chapter 6.

Outline

The thesis will first provide a very brief summary of the relationship between surface science and crystallography, with a clear emphasis on topics that are of particular relevance to the thesis work. This will be followed by a discussion of why material and pressure gaps exist, why they are a problem, and how the work in this thesis can bridge the gaps. Then comes a short introduction to CO oxidation, as this is the model reaction used throughout this thesis. Subsequently, various techniques used in this work will be introduced, including a discussion of how they can be combined. Finally, I will showcase results obtained by combining multiple techniques and provide some outlook on the future of *operando* catalysis experiments.

Chapter 2

Surface Crystallography

In the field of heterogeneous catalysis, the catalytic reactions commonly occur at the surfaces of crystalline metals, more specifically at the so-called active sites, which are places where the reactants can adsorb. Therefore, in this chapter, I will briefly discuss the crystal structure and surface structure of metals, how this relates to these active sites, and how crystallography can help us to better understand how different surface orientations relate to each other.

Metals, oxides, and many other solids are crystalline materials that consist of a repeated set of atoms, the so-called unit cell. Common arrangements of atoms in metals are face-centred cubic (fcc), body-centred cubic (bcc), and hexagonal close packed (hcp) shown in Figure 2.1. Most of the experiments in this thesis were performed on various Pd surfaces. Since Pd has an fcc unit cell, all diagrams will henceforth be for fcc.

The unit cell defines the bulk structure of a compound. However, the compound can be cut in various ways with respect to the orientation of the unit cell. This allows for the

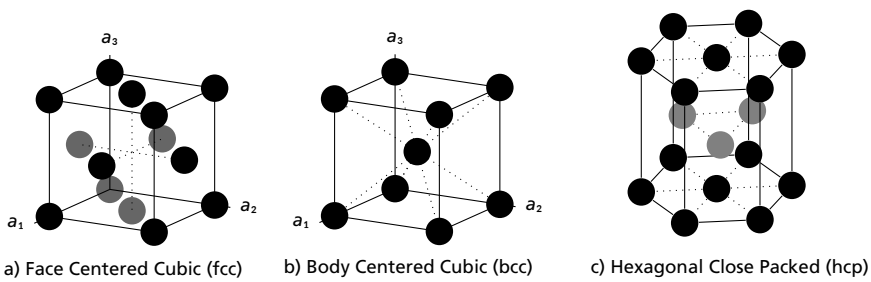

Figure 2.1: The three common unit cells in metals. Pd, the catalyst metal mainly used in this thesis has an fcc lattice as shown in Panel a).

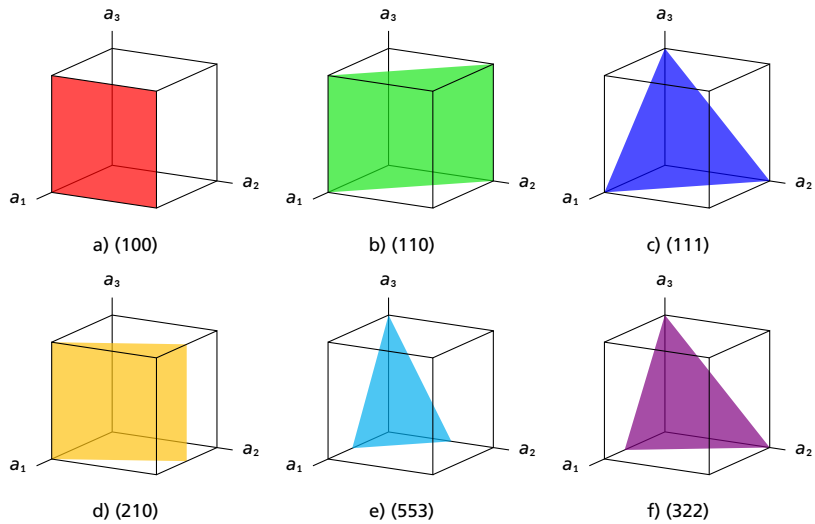

Figure 2.2: The unit cell cut along planes corresponding to various Miller indices. The colors used here match those discussed later in this thesis, and match those in Figure 2.3.

creation of an infinite number of surfaces, which are defined by the orientation of the unit cell with respect to the cut. To denote these surface orientations, this thesis will use both the so-called *Miller indices* common in surface science, as well as a colour coding scheme that is more commonly used in crystallography.

Miller indices specify the reciprocal along the axes of the unit cell, here denoted a_1, a_2 or a_3, where the plane of the cut intersects the respective axis. Zero is taken as the reciprocal of infinity, which in this case means that the cut plane never intersects that axis. This is illustrated in Figure 2.2. For example, the surface in Figure 2.2d is a (210) plane as it cuts a_1 at 1, a_2 at ½, and a_3 at infinity. Panels a–c show the so-called *close-packed* surfaces that contain no steps. All other cuts, for example those in panels d–f, show various *vincinal* surfaces that contain steps, as their cut plane does not pass through the corners of the unit cell. Also, assuming that we have a cubic unit cell, the (100) surface is analogous to the (010) surface and so on — switching any two numbers would simply mean that the unit cell is rotated by 90°.

Although Miller indices work well to unambiguously define a surface and are useful to determine the microstructure of the surface, they do not make it immediately obvious to most people which surface orientations are similar to each other and how two surface orientations are related. Thus, another way to specify surface orientations with colours was developed within the field of crystallography[15]. For the $m\bar{3}m$ symmetry group to which the cubic unit cell belongs, the (100) orientation is red, the (110) orientation is green and the (111) orientation is blue. Any in-between orientation is then assigned a colour, as shown

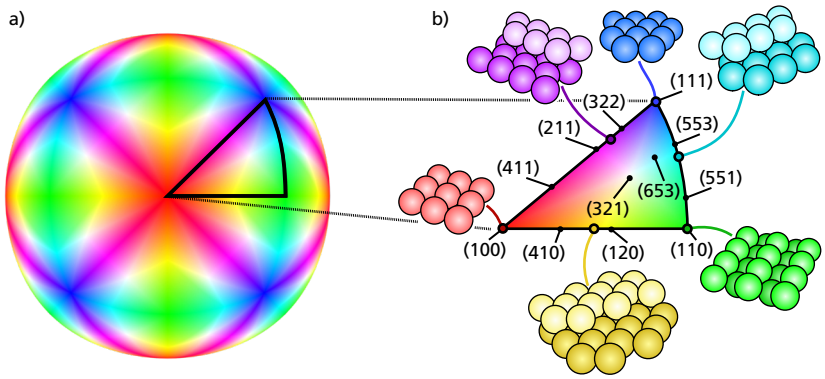

Figure 2.3: The color coding system for surface orientations of a cubic lattice. The idea is that all possible roations of the unit cell are represented as a color. Imagine rotating the ball shown in Panel a) to an arbitrary angle. The colour facing you will then be the colour of that rotation. Now imagine that a crystal is rotated with the ball and cut in the plane of the paper. The surface orientation of that cut then has the color facing you. Panel b) shows examples of surfaces which can be obtained with certain cuts. Note that Panel a) in this figure may look quite different on a computer screen than when printed.

in the coloured triangle — also called the stereographic triangle (ST) or the inverse pole figure — in Figure 2.3. Note that the colours used here correspond to those of the Miller planes shown in Figure 2.2. This triangle can be thought of as the stereographic projection of a coloured ball onto a plane, where the way it is coloured mimics the symmetry of the crystal. For example, rotating the ball 90° to the right will return it to its original state with the red (100) surface facing the reader. However, rotating the ball 90° along the diagonal towards the blue area will rotate the ball past the blue area and result in a green side, the (110) side, facing the reader. This is analogous to the rotations of a cube. Try it out with a Rubik's cube perhaps?

I will now briefly discuss the surface structures that can be obtained by cutting an fcc metal along various planes, starting with the (100) surface. This surface consists of a square pattern that is rotated 45° to the unit cell since two of the corners of each square are, in fact, on the faces of the unit cell. When moving along the edge of the triangle towards (110), we will see (100) surfaces with steps exhibiting (110) microfacets. As we move closer to (110), these steps become longer until what used to be steps is now the surface itself, and the previous surface, in this case (100) will be the shape of the steps. When leaving the edges and moving into the triangle, the edges themselves become stepped, resulting in a so-called kinked surface. A more in-depth discussion of surface microstructure, i.e. steps, kinks and microfacets, and how they relate to Miller indices can be found in ref. 16.

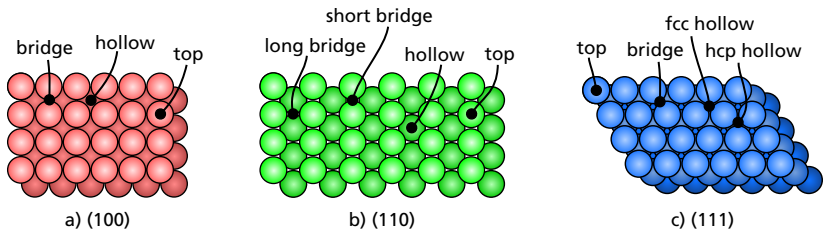

Figure 2.4: The (100), (110) and (111) surfaces and the respective adsorption sites. Note that the (111) surface has two different hollow sites, dependent on the layer stacking below the site.

2.1 Adsorption of Gases

So far we have only discussed the physical properties of the structure of a surface, which are determined by cutting the surface along a certain plane. These give rise to various adsoption sites at which gas molecules can bind to the surface. The most common sites are the on-top, bridge and hollow sites as shown in Figure 2.4. The number of neighbouring atoms is called the coordination number, where sites with a higher coordination number, such as hollow sites or sites at surface steps, have a higher adsorption energy. A higher adsorption energy means that gas molecules will bind more strongly to those sites. Steps also have a higher coordination number as the site at a step is surrounded by more neighbouring atoms. This effect is even more pronounced for kinked steps. Thus, steps play an important role in how gases adsorb onto surfaces[17–19].

Chapter 3

The Gaps to Industry

As mentioned in the Introduction, industry uses large reactors, where the catalyst material is often found in the form of nanoparticles that exhibit a large surface area per amount of material used. These nanoparticles are often carried by a substrate material that can consist of pellets or long channels as shown in Figure 3.1. The pressures and temperatures used in these large-scale reactors are high; for example, the Haber-Bosch process uses pressures of 200 to 400 bar and temperatures of around 450 °C[20].

Substantial information on a catalytic process can be gained from simple studies that can be performed in most industrial reactors. For example, mass spectrometry could be used to analyse the gas at the reactor inlet and reactor outlet. In the hypothetical chemical reaction in which A reacts to C via a potential intermediate B, one could analyse the output for traces of B or attempt to feed only B into the reactor and see if the production of C changes. The isotope marking of certain reactants, such as using ^{13}C instead of ^{12}C, can also be used to study reaction pathways.

However, in order to fully understand the role of the catalyst in the reaction, one needs to understand how the surface of the catalyst material interacts with the reactants and products. To this end, many surface science techniques such as X-ray photoelectron spectroscopy (XPS), low energy electron diffraction (LEED) or high-energy surface X-ray diffraction are available. The crux is that it is very difficult to obtain detailed atomic information without using very simplified model systems under ultrahigh vacuum (UHV) conditions[2]. These techniques are performed in scientific reactors which usually look very different from the huge reactors used in industry. Many measurements are conducted *ex situ* whereby the sample is studied in UHV before and after the exposure to the gases of interest, not during the exposure while the sample is actually active. This allows for detailed studies of the adsorption sites and can be used to relate gas exposure to the resulting coverage. The issue

is that the techniques *ex situ* do not tell us about the intermediate steps, which is especially important when not only studying adsorption, but an actual chemical reaction. Thus, most catalytical reactions are studied *in situ*, where reactants are dosed and products are created by a catalytic process, while surface properties are measured. This can then give information on any intermediate steps. Moving one step further towards industrial realism, we have the *operando* measurements. These are *in situ* measurements performed at higher pressures where it is verified that a meaningful amount of reaction products are produced by the reaction. In this way, more realistic data is produced with the caveat that this usually results in a more complicated experiment. The difference between *in situ* and *operando* is discussed in more detail in ref. 21.

To be able to perform *operando* measurements, we have to create model systems that are as close to the catalysts used in industry as possible while at the same time allowing the use of diagnostic techniques that allow the in-depth study of the catalyst surface and the gas in the vicinity of the surface. Increasingly realistic gas pressure and material conditions require increasingly advanced techniques. Thus, much effort has been invested into creating techniques that can study increasingly realistic samples at higher pressures in increasingly industry-like reactors to bridge the pressure, materials and reactor gaps. This chapter will discuss these gaps and how work done within the scope of this thesis helps bridging them. The techniques mentioned within this chapter are be discussed in more detail in Chapter 5.

3.1 The Materials Gap

If the world was simple, the materials gap would be easy to bridge; it would be straightforward to find out which element the catalytic nanoparticles are made of and just create a larger slab of that element. Then investigate this larger slab using surface science techniques while the reaction is ongoing to see at which phase and which sites the reactants adsorb and react. Unfortunately, the consideration of only the element itself is a simplified picture in which an element is assumed to have only one binding energy per adsorbant. It turns out that the binding energies are quite dependent not only on the surface orientation, but also on the surface coverage, since the various sites on a surface exhibit different binding energies[22]. As the sites with high binding energy become occupied, adsorbants will bind to other, less preferred, sites causing the average binding energy to change. As such, the shape and form of the compound also have an impact on the catalytic activity, since this determines the availability of certain sites. For example, stepped vicinal surfaces, which are not in the very corners of the stereographic triangle, have been shown to play a large role in gas adsorption and catalytic activity[17–19]. It is thus of interest to mimic the multitude of surface orientations exhibited by a nanoparticle using samples that can be studied using surface science techniques.

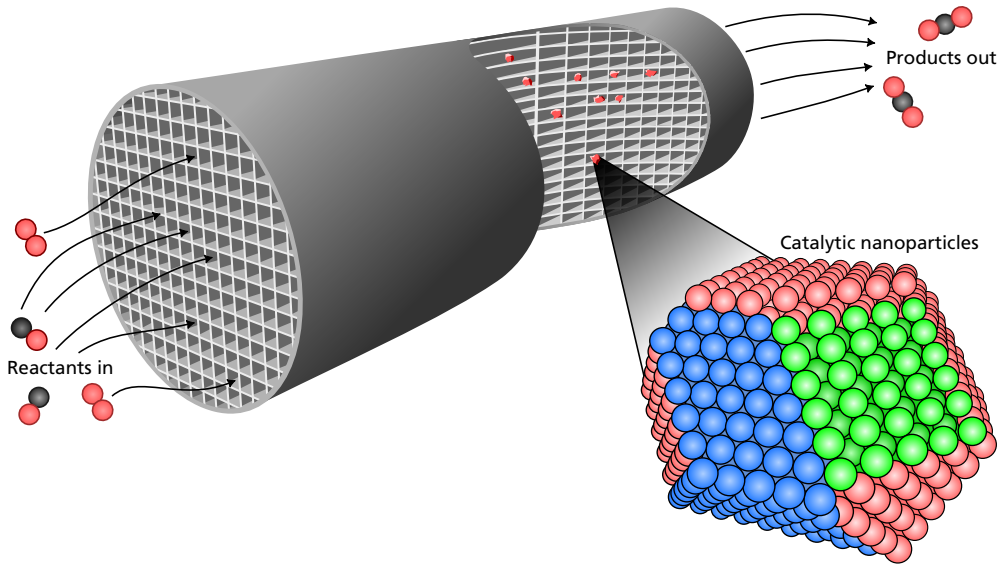

Figure 3.1: Schematic of a catalyst based on industrial nanoparticles. The catalytic nanoparticles are suspended in a tube with many reaction channels through which the reactant gases pass. The nanoparticles themselves expose many different surface orientations. In this case, the nanoparticle exposes facets with red (100), green (110) and blue (111) surface orientations.

In this thesis, no nanoparticle samples have been studied. Instead, the focus has been on technique development to both enable us to better understand simplified single-crystal systems, while also allowing for the use of more complex samples, such as curved crystals and polycrystals, to be studied in great detail. This means probing of both the gas phase and the sample surface with the spatial and temporal resolution needed to follow many processes in catalysis.

3.1.1 Single Crystals

To facilitate the use of surface science techniques and to interpret the results of catalysis experiments to the point where the reaction mechanism can be deciphered, it is important to simplify the surface as much as possible. Thus, in the past several decades, there has been a move toward using single crystals that have a large, well-defined and homogeneous surface with which the reactant gases can interact. These surfaces can then be studied with surface science techniques to better understand the details of where the reactants adsorb and what intermediates are formed[2].

It is possible to use single crystals to emulate a batch of nanoparticles. To do this, the distribution of the facets among the nanoparticles is determined. Multiple single crystals, each

cut in an orientation to model a different facet, are then studied. The combined knowledge gained from multiple experiments performed on multiple single crystal samples can thus be used to model the nanoparticle. For the nanoparticle in Figure 3.1 for example, three single crystals with (100), (110) and (111) orientations would be required. The downside of this approach is that synergies and potential couplings between different facets are not taken into account and effects from atoms at the edges of the nanoparticle are neglected. It may also be experimentally challenging to ensure consistent sample preparation and experimental conditions for all required samples.

The advantage of single crystals is that it should not matter where on the sample one measures, as long as the measurement is performed somewhere on the polished sample surface and the entire surface is exposed the same gas conditions, which is not always the case. In general, single crystals are useful when a well-defined sample is required for use with techniques with limited spatial resolution such as HESXRD or PMIRRAS. Single crystals are also useful when using techniques with spatial resolution on an atomic scale such as Scanning Tunnelling Microscopy (STM) to study a small area of the sample. The entire sample can then be assumed to have a similar surface structure as the small area that was studied with atomic resolution.

In Paper III, we used a well-defined Pd(100) single crystal to demonstrate the usefulness of combining the 2D-SOR, PLIF and HESXRD techniques. The fact that the sample exhibits only one orientation makes it much easier to interpret the diffraction patterns. It also enables us to assume that any variation in surface oxidation or activity is due to an inhomogeneous gas phase.

Even if spatially resolved techniques are available, single crystals are useful. For example, the oxidation of a single crystal Pd catalyst (100) has been shown to depend on reaction-induced gas gradients[13]. In Paper IX, we visualise how gas gradients play a role in the catalytic ignition of the CO oxidation reaction over a Pd(100) single-crystal, which will be discussed further in Chapter 4. In both cases, we can again assume that the sample surface itself is homogeneous and that any inhomogeneities stem from the gas phase composition varying over the sample. Thus, single-crystals are useful when investigating effects where it is useful to be able to exclude variations in surface orientation.

3.1.2 Curved Crystals

Using single crystals has the obvious downside that each sample exhibits only one surface structure, making it impossible to study multiple surface orientations in one experiment without swapping the sample. Depending on the technique, such a sample swap can take significant amounts of time and it is challenging to ensure that experimental conditions do not differ between the samples. Thus, it is of interest to develop samples that exhibit

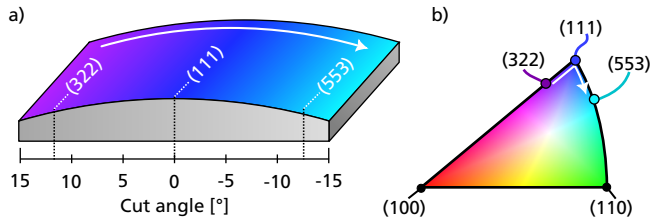

Figure 3.2: Example of the surface orientation continuum that can be created using a curved crystal. Panel a) shows the crystal itself, while Panel b) shows the orientations in the stereographic triangle. The white arrow covers the same surfaces in both panels.

multiple surface structures while still being easy to study.

Recently, curved crystals have been proposed as one solution to this problem. These crystals are first cut in a plane, after which they are curved to expose vicinal surfaces. For example, in Paper **A**, a Pd single-crystal is cut to expose the (111) direction. By subsequently cutting the crystal in a curved shape, it is possible to expose the neighbouring facets. In the ST, this corresponds to going along the edges of the triangle towards the (100) and (110) directions, respectively. By curving it to a maximum angle of 12°, the (223) and (553) surface orientations are exposed at the edges of the crystal, while the centerline keeps its (111) orientation.

The laser-based spatially resolved techniques developed within this thesis have proven to be very valuable in experiments with curved crystals. In this thesis work, we have been able to resolve the individual ignition of each side. For Pt samples, they ignite simultaneously, while for Rh and Pd, one side is clearly more active than the other[**A**, 23, **E**]. However, it should be mentioned that these studies have the flaw that the activity of the already active face will always change the gas conditions at the yet-inactive face through gas diffusion. This spillover effect will affect the ignition temperature of the still inactive face.

3.1.3 Polycrystals

Most metal samples do not naturally form large chunks of single-crystal lattice when produced. Instead, smaller domains with random orientations are formed. This is usually seen as a downside as this means that the surface is ill defined. Many techniques also do not have the spatial resolution needed to adequately resolve individual domains. However, with an adequate domain size, which can be tuned by tuning the metallurgical production parameters, and techniques that can spatially resolve the domains, polycrystals can act as library samples with many well-defined surface orientations that can be studied simultaneously[24–26].

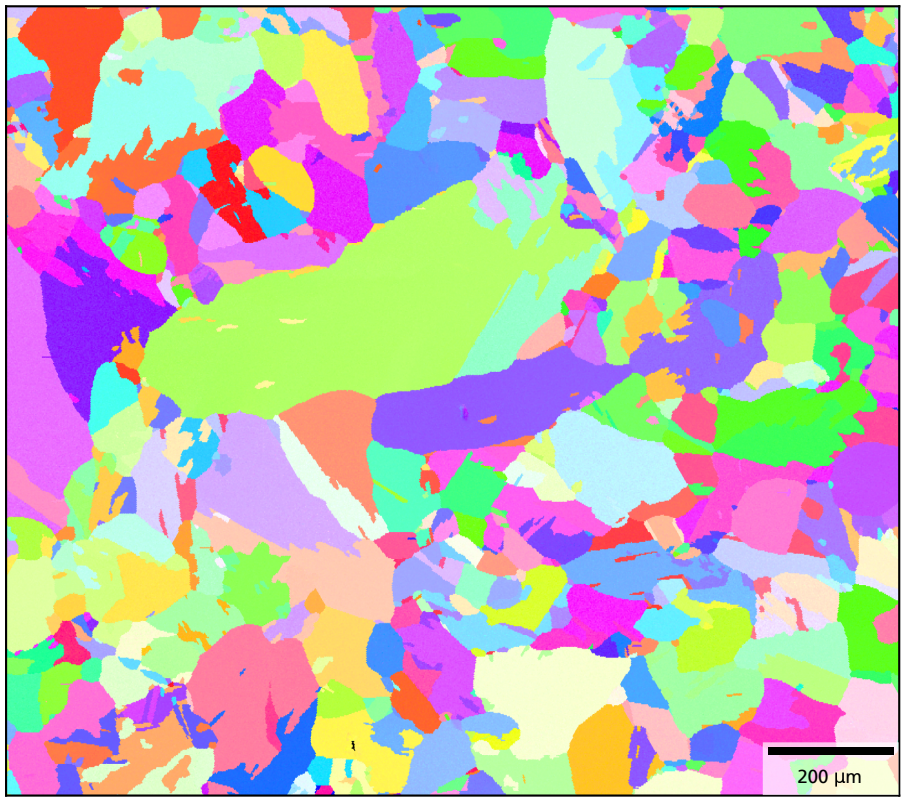

Figure 3.3: The orientations of the polycrystal sample with small grains used in this thesis work as determined by EBSD. Note the diverse distribution of orientations which means this sample can be used as a quasi-continuous library sample exposing many surface orientations. Refer to Figure 2.3 for the color key.

In this thesis, three different polycrystalline palladium samples were used: A piece of Pd foil, a Pd sample with larger grains, and another of similar size with smaller grains. Pd foil, while cheap, turned out to be less useful, as most domains were of similar orientation due to the manufacturing process of foils. The sample with small grains contains a large number of different grains with a wide range of surface orientations that cover large parts of the stereographic triangle. An EBSD mapping of this sample is shown in Figure 3.3. This is also the sample used in Paper VIII. The disadvantage of this sample is that a microscope is required to resolve the individual grains. The mapping of the polycrystalline sample with large grains is shown in Figure 3.4. Although this sample has fewer grains and much of the ST is well represented, it is more difficult to cover the entire orientation space with this sample. The advantage of this sample is that it is large enough to allow for the use of techniques with non-microscopic spatial resolution.

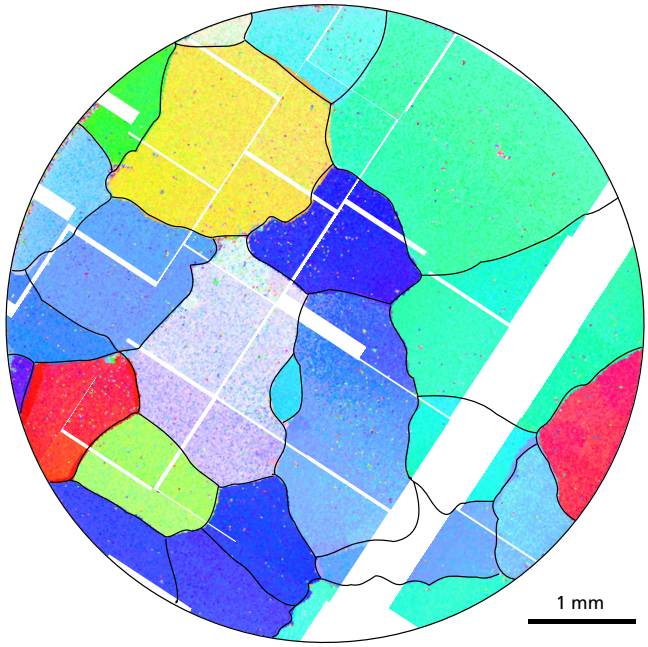

Figure 3.4: An EBSD mapping of the polycrystalline Pd sample with large grains consisting of multiple measurements that have been stitched together. The sample is 7 mm across. While this has fewer grains than the sample in Figure 3.3, the grains are larger which enables them to be resolved with more techniques. For a color key, see Figure 2.3.

Great effort has been spent in this thesis work to develop techniques with a spatial resolution high enough to resolve individual grains. In particular, the 2D-SOR microscope has been very useful in simultaneously monitoring a large number of grains on polycrystalline samples. This is presented in Paper VIII and further elaborated on in Chapter 6. Here, EBSD was used to characterise the surface orientations of all grains within a region of interest (ROI). The same ROI was then monitored with the 2D-SOR microscope.

The disadvantage of polycrystalline samples, except the fact that probing them requires imaging techniques with enough spatial resolution to resolve individual grains to be useful, is that spillover between grains will occur in the gas phase. This will be discussed in more detail in Section 3.2.2.

3.2 The Pressure Gap

Surface science experiments, in which the aim has been to shed light on catalysis phenomena, have historically been conducted at very low pressures. There are two main reasons for this. First, many surface science techniques use electrons as a probe or measure the

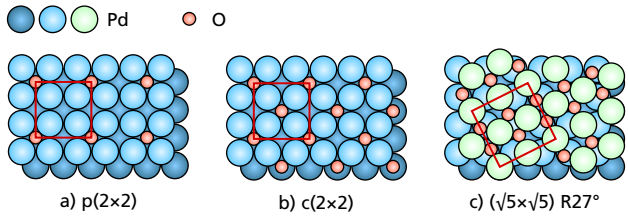

Figure 3.5: Three ways Oxygen can adsorb onto Pd. First, oxygen will occupy the hollow sites in a 2×2 pattern as shown in a). Increasing the oxygen pressure further will result in the center hollow site also being occupied as shown in b). If the pressure is increased even more, a surface oxide forms as shown in c). This surface oxide can then grow into a thicker bulk oxide if the pressure and/or temperature is increased even further.

response of electrons to a different probe. The fact that electrons cannot penetrate into the bulk ensures the surface sensitivity of the techniques. However, electrons cannot penetrate far into high-pressure gas, so the experiments must be conducted at low pressures or use more complicated setups that minimise the path electrons have to travel through high pressure gas. Second, using low pressures ensures a high level of control over the surface structure. Already at pressures of 10^{-6} mbar, the entire sample surface would be covered with adsorbates in seconds, assuming the adsorbates stick to the surface.

However, as the fields of surface science and catalysis become increasingly intertwined and *operando* experiments are performed at higher pressures, the coupling of the surface to the now-existent and relevant gas phase becomes increasingly important to consider. This section will first discuss an example of where pressure matters, even from a surface science point of view. This will be followed by what gas phase properties need to be monitored and what needs to be considered when performing experiments at higher pressures. Discussion of the techniques used to perform experiments at higher pressures will be saved for Chapter 5.

3.2.1 Pressure Matters

In industry, catalysis processes are performed at pressures of up to hundreds of bar, far from the almost deep space-like UHV conditions common in surface science experiments. Gas pressure also has a great impact on the chemical behaviour of the catalyst surface. As an example relevant to this thesis, I will discuss the effect of exposing a Pd(100) surface to O_2. Exposing a clean room temperature surface to O_2 at UHV pressures will result in the binding of chemisorbed oxygen atoms to hollow sites in either a p(2×2) pattern as shown in Figure 3.5a or a c(2×2) pattern as shown in Figure 3.5b[27]. This results in coverages of 0.25 monolayers and 0.5 monolayers respectively, where one monolayer means that there is one oxygen atom for every surface Pd atom. As the O_2 partial pressure is increased, or the sample surface is heated, a $\left(\sqrt{5} \times \sqrt{5}\right)$R27° surface oxide is instead formed with a

coverage of 0.8 monolayers[28, 29] as shown in Figure 3.5c. In this case, the oxide differs from chemisorbed oxygen in that there is oxygen under the Pd atoms. At even higher oxygen pressures, the oxide layer will grow and eventually form a bulk oxide.

This means the surface structure of metals is coupled to the surrounding gas conditions. Hence, monitoring the surface itself if not enough to fully understand the reaction mechanisms at play. They must be combined with simultaneous spatially resolved *operando* measurements of the gas phase. The further development of a suite of techniques that meet these requirements has been a major aim of this thesis work. In Paper III we show how to combine PLIF, 2D-SOR and HESXRD to study surface oxidation while monitoring the surrounding gas phase.

3.2.2 Gas Diffusion

The mean-free-path of a gas molecule, which is the distance it travels on average before changing course due to a collision with another gas molecule, is highly dependent on the gas pressure[30]. As shown in table 3.1, in UHV this mean-free-path is on the order of the distance to the moon. However, it quickly shrinks to around a micrometre under atmospheric conditions. This means that, while one can assume that the entire surface of a mm-sized sample is exposed to the same gas conditions when performing experiments at UHV, this is no longer the case for measurements at mbar pressures or higher. In Paper V we investigated how the gas cloud around a catalyst behaves with varying pressure and flow rates. We show that the gas concentration gradients become increasingly steep as pressure increases; an example of this is seen in Figure 3.6. For completeness, the mean-free-path of commonly used gas molecules at various pressures is presented in Table 3.1.

Thus, to be able to understand the correlation between surface structure and gas composition at high pressure conditions, point measurements of the gas concentration with techniques such as mass spectrometry are not sufficient; The gas composition will exhibit spatial variations that can vary quickly as the sample activity changes.

Gas diffusion between parts of the reactor can also affect the sample surface and the catalytic activity, which is shown in Paper IX. Here, we show that the catalytic ignition is in fact driven by gas gradients in the reactor, and as a small part of the sample becomes active, the resulting gas conditions in the active area diffuse to other parts of the sample. This results in rapid ignition of the entire sample. More discussion on the catalytic ignition can be found in Section 4.2.1.

Table 3.1: Mean free paths at 300 K for various pressures according to eq. 4.3a in [30]. Note that at UHV the mean-free-path is almost a light second, between 200 000 km and 300 000 km.

	CO_2	CO	O_2	N_2	CH_4	Ar
UHV (10^{-10} mbar)	0.9 ls	0.7 ls	0.8 ls	0.73 ls	0.7 ls	0.8 ls
HV (10^{-6} mbar)	270 m	208 m	245 m	221 m	203 m	254 m
1 mbar	2.7 cm	2.1 cm	2.4 cm	2.2 cm	2.0 cm	2.5 cm
100 mbar	0.27 mm	0.21 mm	0.24 mm	0.22 mm	0.20 mm	0.25 mm
1 bar	27 µm	21 µm	24 µm	22 µm	20 µm	25 µm
300 bar	90 nm	70 nm	81 nm	73 nm	68 nm	84 nm

3.2.3 Gas Temperature

As the gas pressure surrounding the catalyst increases, it becomes relevant to also measure the temperature of the gas in the reactor. This is especially important in cases where the sample is not heated directly but by the incoming gas flow. Within the scope of this thesis, we have looked at possible ways to use PLIF to measure the temperatures in the reactor. This work is presented in Paper VI and the techniques are further elaborated in Chapter 5.

3.3 The Reactor Gap

The potentially greatest gap between catalysis research and industry is the reactor gap. When reactors are developed for fundamental catalysis research, instead of starting from an industry reactor and then modifying it to allow more fundamental studies, reactors originally designed for fundamental surface science experiments have been adapted to work with higher pressures and support *operando* experiments. Here, the choice of technique is the primary factor, and the reactors are built around a certain diagnostics technique. Industry reactors, on the other hand, are naturally constructed to maximise the production of products, with little concern for being able to study the reaction itself in the detail needed to draw conclusions on the fundamentals of the reaction mechanism. This reactor gap makes it challenging to transfer the knowledge gained from fundamental research reactors to industry.

In combustion research, this problem has been solved by approaching the issue from the other side, namely by adapting industry reactors, aka engines, to allow for them to be extensively studied using scientific techniques. For example, large resources have been spent on development of so-called optical engines, where — and this is key — *existing* engines are modified and fitted with glass windows. There have even been instances in which glass cylinders have been developed to allow *operando* fuel injection measurements, etc. While these modifications slightly alter the behaviour of the engine, it is still similar enough to be able to draw conclusions that directly transfer over to real engines. In combustion research, existing reactors were adapted and techniques were chosen to accommodate this. These

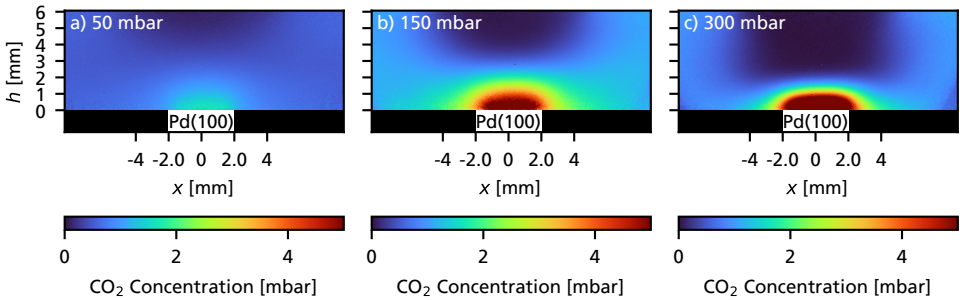

Figure 3.6: Gas diffusion at different pressures. The figure shows the CO_2 gas cloud surrounding an active Pd(100) catalyst at 50 mbar (a), 150 mbar (b) and 300 mbar (c). In all cases, the feed gas is introduced from above. Note that higher pressure results in sharper gas gradients.

techniques have been developed to allow increasingly fundamental conclusions to be drawn.

Perhaps the way to go is to meet in the middle. Of course, the work done to adapt surface science reactors to work at higher pressures should continue. However, simultaneously efforts should be made to find surface-sensitive techniques that can be used in modified industry reactors. In this thesis, optical techniques have been developed that could be candidates for this, but there may be other better-suited techniques. More work, money, and much trial-and-error will be needed to find the optimal solution to this issue.

Chapter 4

Catalysis and CO Oxidation over Pd(100)

Since this thesis is heavily focused on the development of techniques, most of the experiments carried out within the scope of the thesis use catalytic oxidation of CO to CO_2 with a Pd catalyst as model reaction. This reaction is chosen because it is a very simple and intensively studied reaction with much literature to fall back on[14]. At the same time, some details of the reaction mechanism are still unknown, especially at higher oxygen pressures.

4.1 Why Pd and the Volcano Plot

In order to work as a catalyst at all, a compound has to react with the reactants and then restore itself to be ready to react with more reactant. Thus, we are interested in compounds that are reactive enough for the reactants to stick to them, changing some bonds to allow a reaction to occur but not so reactive that the products will keep sticking to the catalyst. This is summarised by the Sabatier principle, whereby the catalytic activity of a compound is highly dependent on the binding energies of the reactants to that compound. Often a so called so-called *volcano plot* is used where the rate is plotted against the binding energy of one or more reactants. Figure 4.1 shows an example of this graph for CO oxidation. As can be seen, the transition metals Pt, Pd and Rh are among the most catalytically active, which is why they are often used as catalysts in oxidation reactions[31, 32]. The high reactivity of these transition metals is explained by the d-band theory[33]. A d-band with a large density-of-states close to the Fermi level results in a high reactivity, which is the case for the transition metals. In this thesis, Pd catalysts will be used.

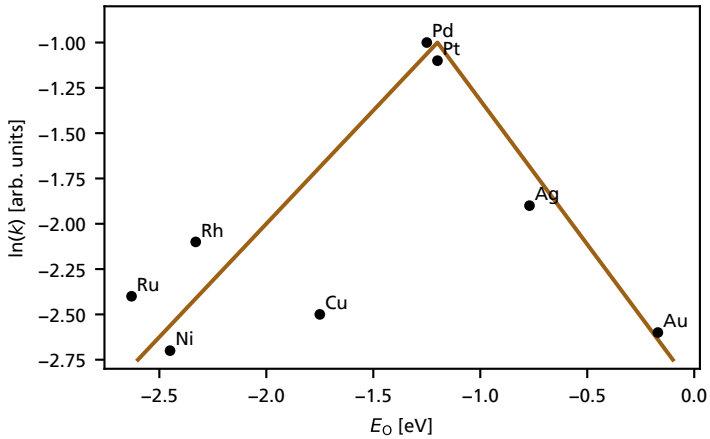

Figure 4.1: So-called Volcano plot for the CO oxidation reaction. From the plot it is clear the the transition metals Pd and Pt have the highest activity. The data is from ref. 22.

4.2 The Arrhenius Equation and CO Oxidation

From statistical mechanics and thermodynamics, we know that the probability that a particle has a certain energy depending on its temperature is

$$P_E \propto e^{-\frac{E}{k_B T}}.$$

If the activation energy of a chemical reaction is E_a, the reaction rate k is thus

$$k = A \cdot e^{-\frac{E_a}{k_B T}}.$$

Taking the logarithm of both sides yields

$$\ln(k) = \ln(A) - \frac{E_a}{k_B} \cdot \frac{1}{T}.$$

We thus get a linear equation where $\ln(k)$ is linearly dependent on T^{-1} with a slope of E_a/k_B. This is the form in which catalysis data is most commonly plotted.

Figure 4.2 shows an example of a catalytic CO oxidation experiment on Pd(100) in which the sample temperature is increased over a period of 15 minutes. The same data as is plotted in Figure 4.3 where the activity is plotted against the inverse of temperature. We observe an exponential increase in catalytic activity as the temperature is increased. This is followed by a sharp and sudden increase, called catalytic ignition. The sample activity then reaches a plateau as the reaction becomes limited by the diffusion of gas to and from the sample surface.

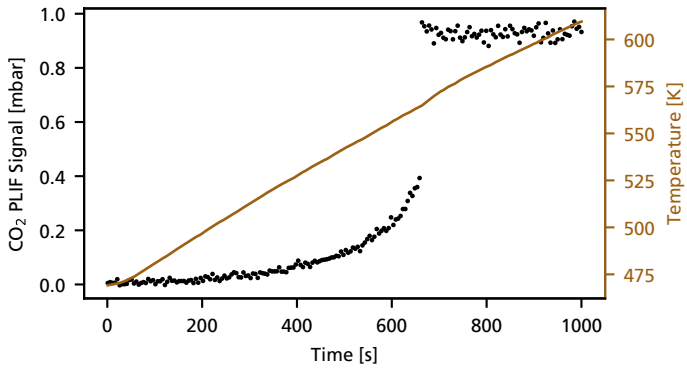

Figure 4.2: An example measurement which shows the measured catalytic activity in form of the CO_2 production as the sample temperature is increased over time. In this case, the CO_2 concentration is extracted from the PLIF data in Paper **A**.

This shows that we must separate the *intrinsic* activity of the sample, which is mainly dependent on temperature, from the actual turn-over frequency, which is dependent on both the intrinsic activity of the sample and other parameters such as gas diffusion within the reactor and the state of the sample surface.

There are three proposed reaction mechanisms for CO oxidation on Pt-group metals. First, the *Langmuir-Hinshelwood* mechanism by which both O_2 and CO first adsorb to the clean metal surface. The O–O bond is weakened in the process, allowing the adsorbed CO to react with one of the O-atoms to form CO_2. In the *Mars-van Krevelen* mechanism, CO reacts with an already formed surface oxide, reducing the oxide while picking up an oxygen atom, resulting in the production of CO_2. This requires that an oxide has been previously formed. Finally, there is the *Eley-Rideal* mechanism, which is similar to *Langmuir-Hinshelwood*, the difference being that only the O_2 molecules ever adsorb on the surface, the CO molecules react directly from the gas phase without ever spending any time on the surface.

While the sample is inactive, literature suggests that the surface is covered in CO, making it impossible for any oxygen to adsorb, inhibiting all three reaction mechanisms. As the surface is heated and CO begins to desorb, some oxygen can reach the surface and react.

4.2.1 The Catalytic Ignition

From looking at Figure 4.3, it is evident that the measured trend deviates from the fitted trend line just before the catalytic ignition. So what is going on here? The catalytic ignition was first defined around the ignition temperature, which is the temperature at which the heat created by the exothermic reaction is greater than that which can dissipate from the sample, causing the sample temperature and sample activity to rapidly increase[34]. This

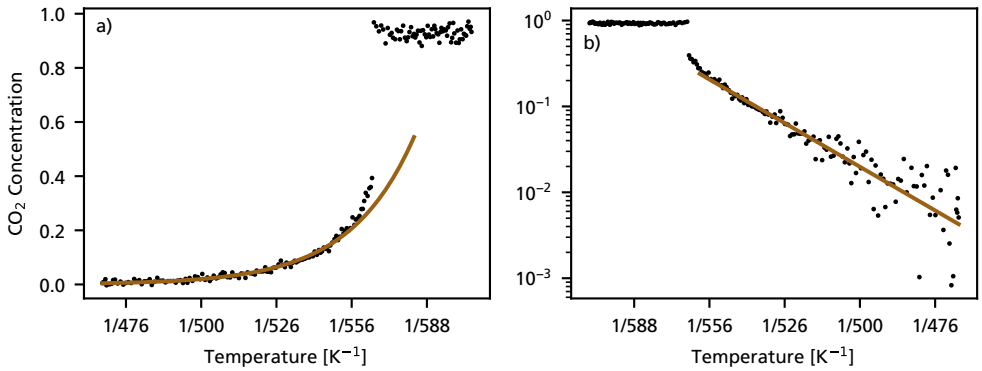

Figure 4.3: Results from a typical CO oxidation measurement where the CO production is plotted as function of inverse temperature. Both plots show the same data. The right plot uses a normal *y*-axis and a reversed temperaute axis, whereas the left panel shows an Arrhenius plot.

rapid increase then coincides with a transition from the kinetic reaction regime, where the reaction rate is limited by the intrinsic catalytic activity, to the diffusion-limited regime[34]. Here, the surface is so active that any gas reaching the surface will react — the actual activity is limited by the rate at which reactant gas can diffuse to the surface. Since then, similar transitions from low to high catalytic activity have been shown to occur at certain threshold temperatures, also under UHV conditions, where the temperature increase from the exothermic reaction can be neglected[35]. This is explained by temperature-induced changes in the surface structure or composition that change the intrinsic surface activity. Using Pd(110) as an example, this means a transition from a CO-covered metal surface, where oxygen cannot react, to an oxygen-covered surface as enough CO has been thermally desorbed from the sample to allow oxygen to adsorb and react [36]. Paper IX, which is summarised in Section 6.2, discusses this in detail and shows how the catalytic ignition is affected by performing *operando* experiments at higher pressures.

Chapter 5

Techniques and Equipment

This chapter will focus on the optical techniques that were developed and applied in this thesis. Following this, other techniques will be introduced that were combined with the optical techniques. I will also discuss experimental equipment, such as the reactor used in the catalysis experiments. A schematic showing the reactor, gas system, lasers, optics, and detection equipment is shown in Figure 5.1.

5.1 Reactor and Gas System

All experiments in this thesis were performed in a ~23 cm^3 flow reactor originally manufactured by Leiden Probe Microscopy, which is strongly inspired by the high pressure part of the design presented in [37]. The reactor consists of a cross-shaped resistive heater which also acts as sample holder surrounded by a stainless steel enclosure with optical access. To ensure that the heater remains chemically inert, any exposed surface is covered with boron nitride (BN). Ta screws and nuts, which do not easily oxidise under oxygen-rich conditions, attach the heater to the reactor base. The heating current is set by a computer-controlled power supply that can either be configured to ramp the current at a fixed rate or use a PID to instead ramp the temperature at a fixed rate by adjusting the current. To monitor the temperature of the heater, a thermocouple is attached to one end of the cross. The calibration of the sample and gas temperatures with respect to the thermocouple temperature are presented in Paper VI. Water cooling of the reactor base ensures a stable operating temperature. The reactor top can be exchanged depending on the application. In this thesis work, four different tops were used. First, a five-way optical access top, which is a stainless steel cube with five 17 mm diameter access ports, one on each side and one on the top. These access ports can be equipped with windows for optical access or gas pipes to allow

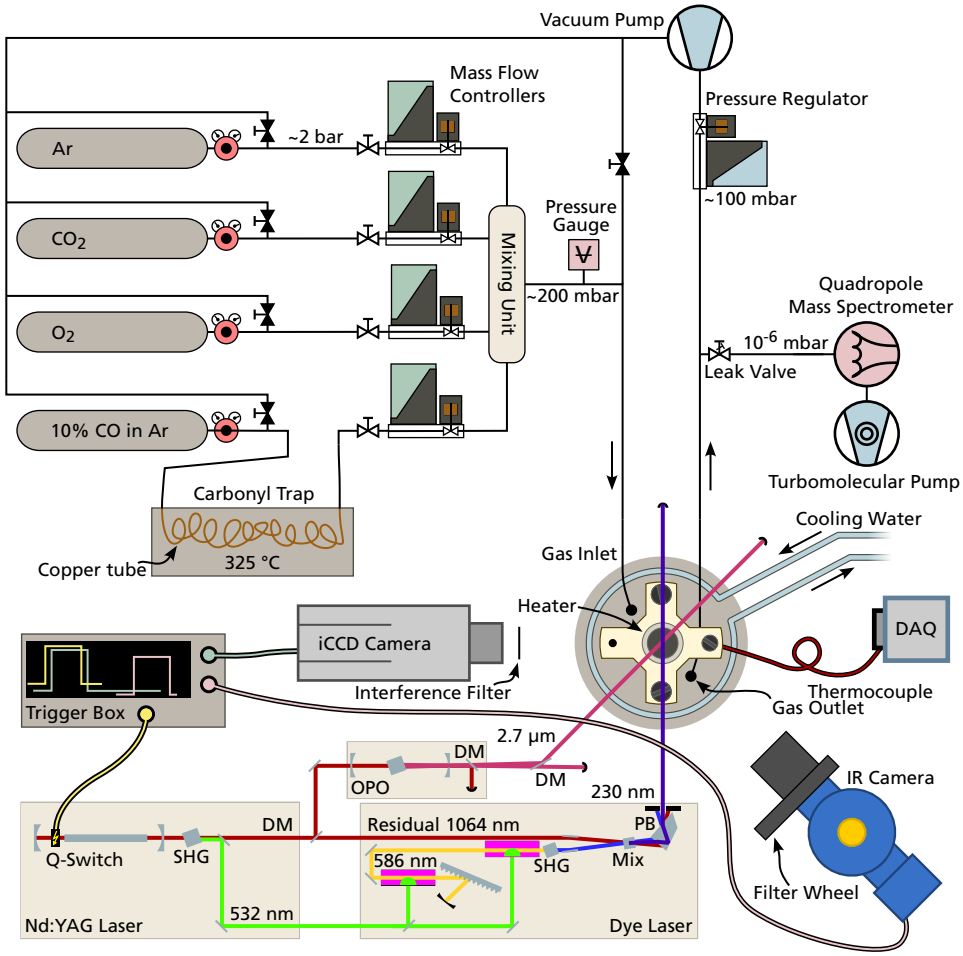

Figure 5.1: A schematic of the experimental setup showing the reactor, the gas system, the laser system and the two cameras used to detect the PLIF signal. The gas valves that are open during normal operation are white whereas those only used for pumping the reactor or gas lines are black. The 2D-SOR setup is not shown, for this, refer to Figure 5.13.

for different flow configurations as shown in Figure 5.2. The stagnation point flow where the gas is introduced from above resulting in a symmetric gas distribution is particularly useful, as it is easier to perform flow simulations that way. Another variant with nine ports, eight on the sides and one on the top, was also used. To reduce reflections, we covered the interiors of the stainless steel enclosures, which do not reach very high temperatures, in graphite spray. For diffraction experiments, it is desirable to be able to rotate the reactor. To allow this, two transparent cylindrical enclosures were produced, one made of sapphire, which transmits mid-IR, and another made of fused silica, which is suitable for the UV range.

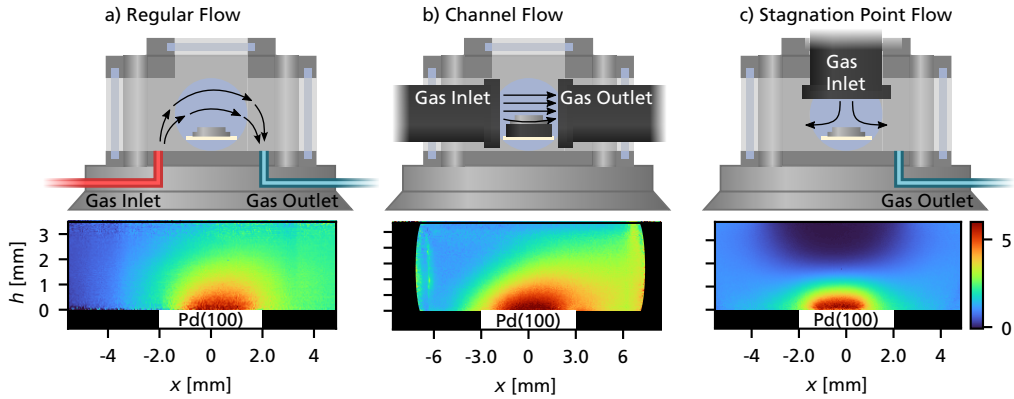

Figure 5.2: Different flow configurations give rise to different gas distributions in the reactor as shown here with PLIF during CO oxidation over a Pd(100) sample at around 150 mbar. This means the sample surface is exposed to different gas conditions, even if pressure and gas mixture are equal. In the regular flow (a), the gas is introduced from below in a less controlled manner resulting in a rather wide cloud. In channel flow (b), the gas is introduced such that it flows parallell to the sample surface. In this case the sample is raised to place the surface in the center of the gas flow. In stagnation point flow (c), the gas is introduced symmetrically from above.

The gases used for the experiments are stored in gas bottles with pressure regulators that keep the outflow at around 2 bar. Flow rates into the reactor are controlled by a set of Bronkhorst El-Flow Mass Flow Controllers (MFC). Behind the flow controllers, there is a mixing chamber to ensure a homogeneous gas mix at the reactor. The MFCs are computer-controlled to allow for logging of the gas flows. Within the scope of this thesis, custom software was developed that enables the use of automated linear ramps of gas flows during measurements. The pressure in the reactor is set by a Bronkhorst El-Press pressure controller placed between the reactor and a vacuum pump. To ensure that the gases in the reactor are as pure as possible, the same vaccum pump is also connected via valves to the gas lines from the gas bottles, to allow for pumping the gas lines. Two pressure gauges are present in the setup. One measures the pressure after the mixing unit and the other is the pressure controller which also acts as a pressure gauge. Calibration measurements show that the reactor pressure is the average of the pressures reported by these two gauges. This also makes sense from a physical point of view, as the gas pipes at the reactor inlet and outlet are of the same diameter when using the reactor in the regular flow configuration. Since CO is used in the reactions, a carbonyl trap is used to remove any carbonyls formed by chemical reactions between the CO and the gas bottle or gas regulator. This trap is placed such that all CO gas passes through the trap before entering the MFC.

To analyse the gas exiting the reactor, a quadropole mass spectrometer (Pfeiffer QMG 220) is connected to the gas outlet via an automatic leak valve. This leak valve keeps the pressure in the mass spectrometer at 10^{-6} mbar. The data from the mass spectrometer is logged together with the gas flows, the sample heating current and the sample temperature.

5.2 Laser Systems and Detectors

Tables 5.1 and 5.2 show some technical details of the lasers and cameras used that were used in this thesis work.

Table 5.1: The lasers used in this thesis work, including intermediate mixing stages. All lasers were pumped by a pulsed 10 Hz Nd:YAG laser. The output of the Continuum Vista dye laser depends on which dye is used. The linewidths are taken from the manual of the respective laser.

Model	Type	Tuning Range	Used Output	Energy	Linewidth
Continuum PL 8010	Nd:YAG	—	1064 nm	1.5 J	0.003 cm^{-1}
Continuum PL 8010	Nd:YAG SHG	—	532 nm	800 mJ	0.003 cm^{-1}
Continuum Vista	Dye	380 – 980 nm	586 nm	150 mJ	0.05 cm^{-1}
Continuum Vista FX	SHG & Mixing	216 – 980 nm	230 nm	~10 mJ	0.05 cm^{-1}
GWU versaScan-L	OPO	1.5 µm – 3.6 µm	2.7 µm	~25 mJ	~20 cm^{-1}

Table 5.2: The cameras used in this thesis work.

Detector	Resolution	Wavelength Range	Cooling
Santa Barbara Focalplane 134	256×256 px	1 – 5 µm (without filters)	Liquid N_2
Andor iStar CCD	1024×1024 px	270 – 800 nm	Air
Andor Zyla sCMOS	2048×2048 px	400 – 900 nm	Air
IDS UI-3260CP	1936×1216 px	400 – 800 nm	None

5.3 Planar Laser Induced Fluorescence PLIF

Laser-based techniques are well-suited for gas diagnostics, and many different laser-based techniques have been developed with a variety of applications in mind[38]. The main advantage of laser-based techniques is that they can probe without any physical object being present at the probing location. This means that they do not disturb the gas flow or gas temperature, and no additional compound is added to the reaction system to be studied. The techniques also have high temporal resolution, as the lasers used can be, and often are, pulsed with nanosecond or even femtosecond pulse lengths. Even if the fluorescence has a small delay, as is the case when vibrational transitions are used, this is usually within tens of µs which is still faster than most diffusion processes at ambient pressures. Note that the temporal resolution is not the same as the repetition rate. The temporal resolution defines how "smeared out" each image is in the temporal domain, while the repetition rate determines how often a dataset can be captured.

One of the primary techniques used and further developed in this thesis work is Laser Induced Fluorescence (LIF). The principle behind this technique is that a laser, which is tuned to target a transition in the gas species to be probed, irradiates the probe volume, exciting the gas molecules. A detector is then used to detect the radiation that is emitted

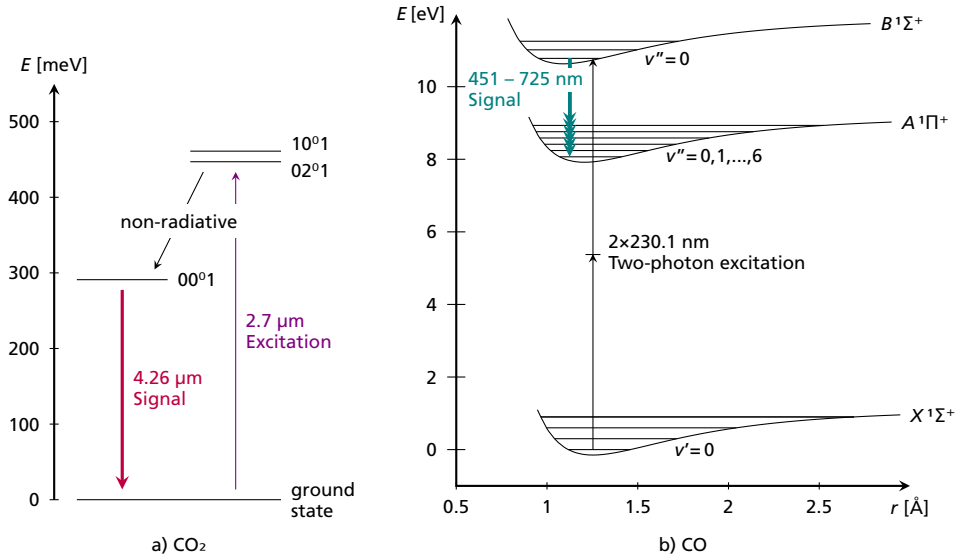

Figure 5.3: Energy level diagrams showing the excitation scheme used for CO_2 (a) and CO (b). The energy level data is taken from ref. 39.

from those molecules as they de-excite via spontaneous photon emission. If a cylindrical lens are used to form the laser into a planar sheet in the area to be probed, and a camera is used to collect the fluorescence, the technique is referred to as Planar Laser Induced Fluorescence (PLIF), which also has spatial resolution. The resolution in the z-direction, defined as the direction perpendicular to the sheet, is then determined by the thickness of the laser sheet, while the resolution in the x and y directions is determined by the resolution of the camera and the imaging optics.

In this work, PLIF was used to detect CO and CO_2 in the vicinity of working Pd catalysts converting CO to CO_2. The laser setup used to do this is described in Paper I, but I will also elaborate a little on the setup in this chapter.

5.3.1 CO_2 Detection

Due to a lack of easily accessible transitions in the UV or visible range, the detection of the CO_2 molecule must be performed using one of the strong vibrational transitions in the mid-infrared. There are three major transitions of interest: The very strong fundamental band at 4.3 µm, and two combinations bands at 2.0 µm and 2.7 µm respectively[39–41]. The disadvantage of using the band at 4.3 µm, is that the strong cross section also results in very strong absorption of the incident laser beam in the air between the laser and the reactor. The band at 2.0 µm is rather weak, leaving the band at 2.7 µm as a good middle

ground. CO_2 molecules excited by 2.7 µm photons initially decay nonradiatively to an intermediate state, after which they decay to the ground state emitting 4.26 µm photons as shown in Figure 5.3a.

To obtain 2.7 µm laser pulses for CO_2 detection, the output of a 10 Hz pulsed Nd:YAG laser (Continuum Powerlite DLS 8010) at 1064 nm was used to pump an Optical Parametric Oscillator (GWU versaScan-L 1064). This is another laser consisting of a cavity with a nonlinear crystal as lasing medium. The OPO outputs two beams at different angles, the so-called signal and idler beams. The ratio between these can be tuned by rotating the crystal with respect to the incident beam, whereby the sum of the photon energies of the signal and idler beams is equal to that of the pump beam[42]. The OPO is tuned so that the idler beam targets the vibrational combination band in CO_2 at around 2.7 µm. The resulting flourescense centred around 4.26 µm is detected using an LN_2-cooled IR camera (Santa Barbara Focalplane 134) with a 256×256 px resolution. The decay time of this transition is very long at around 80 µs, depending on quenching and other effects, see Figure 5.11 for details. The camera exposure is set to around 20 µs to balance signal strength and thermal background. A delay of 10 µs is used to avoid any direct laser reflections, and to ensure that the fluorescence has reached its full intensity. This is shown in Figure 5.4. To reduce the thermal background, a bandpass filter centered at 4.26 µm is used.

In this thesis work two different triggering schemes of the laser and camera were used. In the primarily used triggering scheme shown in Figure 5.4a, the camera is triggered once for every laser pulse and once between laser pulses to record background images. This means that there is a 50 ms delay between the signal and the background. This is sufficient for most use cases. However, at the catalytic ignition of the sample, the sample heats rapidly, which means that it is of great importance to obtain the background with as little time delay as possible. Therefore, to study catalytic ignition, another triggering scheme was used where the camera was triggered at 200 Hz, as shown in Figure 5.4b. This results in 19 background images for every image with fluorescence, with the next background image being only 5 ms delayed. The temperature data itself can also be used for thermography, which is discussed more in Section 5.4.1.

Figure 5.5 shows excitation scans obtained by using a stepper motor to linearly manipulate the angle of the nonlinear crystal in the OPO while recording the fluorescence with the IR camera. The scans were taken at sample temperatures of 280 K and 650 K, respectively. By selecting a region-of-interest in the PLIF images just above the sample, we can assume that the gas is at a similar temperature. The figure also shows simulated spectra from the HITRAN database for the two temperatures[43, 44]. The data match fairly well; however, the OPO output seems quite wide and possibly even contains a frequency comb, resulting in beating patterns in the acquired spectra.

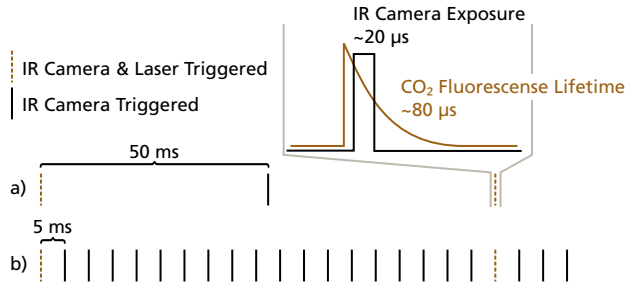

Figure 5.4: The triggering schemes used for CO_2 detection. The camera is either triggered once (a) or 19 times (b) between laser shots in order to acquire the thermal background. The trigger of the camera is delayed around 10 µs with respect to the laser.

5.3.2 CO Detection

In contrast to the CO_2 detection scheme, which uses vibrational transitions, an electronic transition from the $X^1\Sigma^+$ ground state to the $B^1\Sigma^+$ state is used to detect CO. This transition lies deep in the UV and is reached through two-photon excitation at 230.1 nm[45, 46]. The 230.1 nm beam was created by using the second harmonic of an Nd:YAG laser (Continuum Powerlite DLS 8010) at 532 nm to pump a dye laser (Continuum Vista). The dye laser output was tuned to 586 nm. The second harmonic of the dye laser was then mixed with the residual of the Nd:YAG at 1064 nm resulting in a 230 nm beam. The resulting fluorescence emitted as the molecule decays to the various vibrational levels of the intermediate $A^1\Pi^+$ state is in the 450-700 nm range. This fluorescence was imaged using an intensified CCD Camera (Andor iStar). To reduce the background, a multi-bandpass interference filter is used. This filter has several transmission bands, each centred on a CO line.

Although there is no thermal background in this case, the fluorescence for this transition is immediate, and thus reflections from the incident laser cannot be "gated away" by simply delaying the camera exposure. Instead, the laser was detuned from the transition, after which background images were acquired. These could then simply be subtracted from the data images. An excitation scan, in which the dye laser was scanned, is shown in Figure 5.6.

5.3.3 Data Analysis

When the raw data images have been collected, several steps are required to obtain the final spatially resolved concentration images. We first have to conclude that the counts recorded by the camera represent not only photons originating from fluorescence but also background and instrument noise.

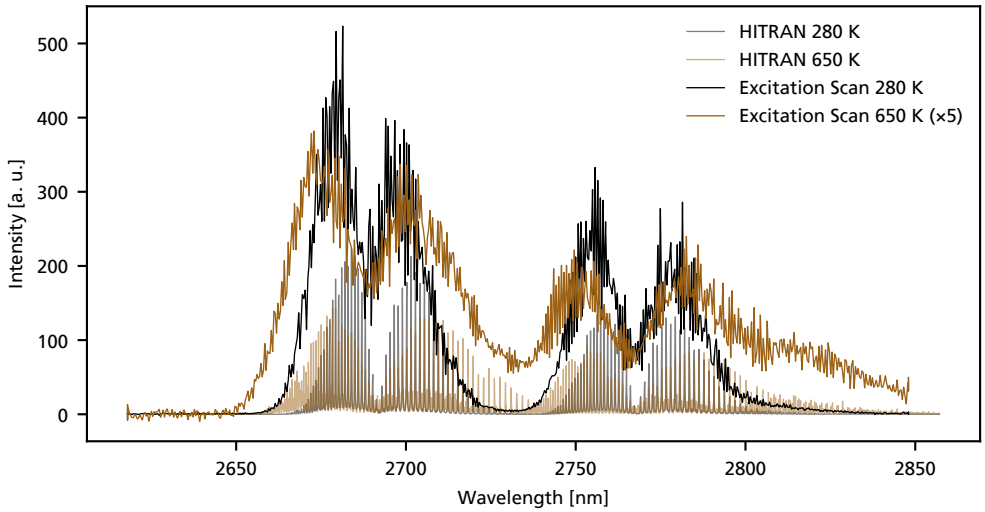

Figure 5.5: Excitation scans of CO_2 at 280 K and 650 K using the OPO. The clean specta as provided by HITRAN are also plotted for comparison.

In all, the fluorescence intensity I at a point x as the laser strikes the probe volume can be expressed as

$$I = Egf(T(x))\sigma_0 N(x)\phi,$$

where E the laser energy, g the spectral integral between the laser frequency distribution and the targeted lineshape, $f(T(x))$ the Boltzmann fraction of electrons in the ground state of the targeted transition at temperature T, σ_0 the absorption cross section, N the number density of the gas to be probed and ϕ the fraction of gas molecules that decay via photon emission. Here, it should be noted that the partial pressure and the number density are related through the ideal gas law. The number density decreases with increasing temperature in isobaric systems such as the reactor used in this work.

When placing a camera to image the fluorescence outside of the reactor, the counts of each pixel in the raw image R actually recorded by the camera are then

$$R = I \cdot G(y)\eta_c \int_0^l f(T(x))N(x)\sigma_0 \mathrm{d}x + B,$$

where $G(y)$ is a factor due to geometry, η_c is the camera collection efficiency at the fluorescence wavelengths that could vary over the sensor, the integral is self-absorption according to the Beer-Lambert law. The last term B is the total background, which are any counts not originating from fluorescence.

Background subtraction is the first step in the data analysis. For the CO case, this is straightforward as the background is temperature-independent and can be obtained once for every

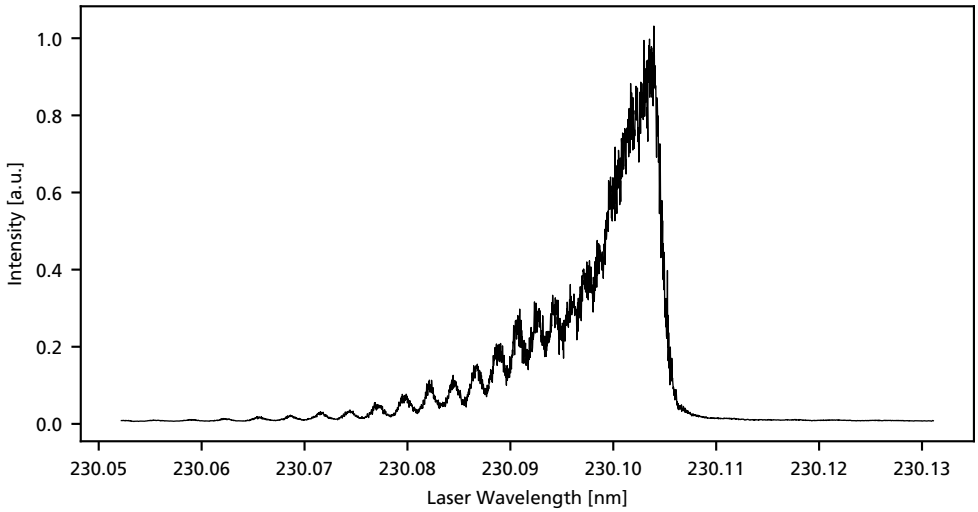

Figure 5.6: Excitation scan of the region around 230.1 nm, which is the wavelength of the two-photon transition used to excite the CO.

dataset by simply detuning the laser away from the CO transition wavelength. CO data and background images are shown in Figure 5.7.

In the case of the CO_2 signal, background images are taken continuously as mentioned above. The closest background image taken before or after the respective PLIF image is then chosen as the background image for that specific data image. Thus, each data image has its own unique background image. The background is also much larger here, accounting for most of the camera counts, as shown in Figure 5.8. In fact, it is difficult to even distinguish the data and background images since the actual signal is so weak.

Next, there are a number of other parameters that can be controlled using a reference measurement, in this thesis also referred to as profile measurement. To perform this measurement, the entire reactor is filled with the gas to be detected, in this case CO or CO_2. PLIF images are then acquired at various sample temperatures. This is done in one of two ways. The first way is to acquire these profile images while a temperature ramp is performed, analogously to that performed under reaction gas conditions. The second, which is used in situations such as synchrotron beam times where time is limited, is to take profile images only at the maximum and minimum temperatures of the range to be used. A function can then be fitted on a per-pixel basis to interpolate between temperatures.

When the images acquired under reaction conditions are divided by the profile images while keeping the same camera position, many of the parameters cancel. This is shown in Figure 5.9. The parameters that fully cancel are the collection efficiency η_c, any geometric

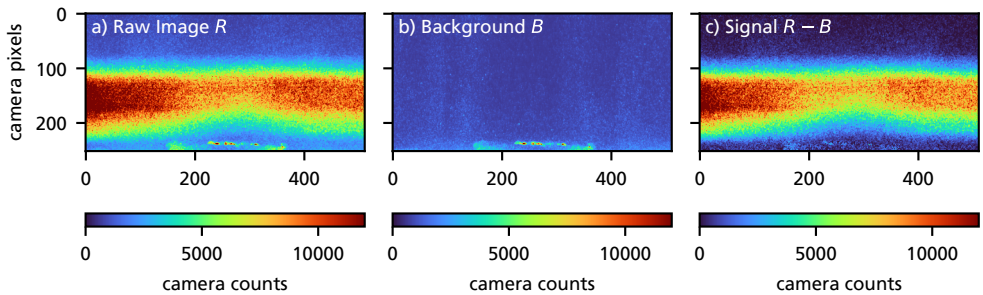

Figure 5.7: CO PLIF Background Subtraction. Panel a) shows a raw fluorescence image, and Panel b) shows a background image taken after detuning the laser away from the transition. Panel c) shows the data in Panel a) after the background has been subtracted. The bright line at the bottom center of the images light scattering off the sample. Note the much smaller background compared with the CO_2 case in Figure 5.8.

factors G arising e.g. from less light reaching the sensor from close to the sample. The absorption in the air outside the reactor also cancels out, assuming that the air in the lab does not change to a large extent. The main absorbers in this case are water and CO_2, so the lab humidity must be controlled throughout the measurement.

Many other parameters cancel to a large extent. The first of these are the inhomogeneities of the laser sheet. While shot-by-shot variations cannot be accounted for, the general spatial profile of the laser sheet will cancel. The temperature-dependent number density N and the ground state population $f(T(x))$ also need to be accounted for. These cancel, assuming that the temperature distribution in the gas is the same during this profile measurement as during reaction conditions. Although this is not fully the case, the gas mixture is different after all, with different thermal properties, it is close enough.

The factors that are left to discuss are the self-absorption within the reactor, as well as any quenching ϕ, which depends on the gas mixture and is discussed more in Section 5.3.4. The self-absorption could be corrected by assuming a spherically symmetric cloud, using the concentration data in the x and y directions to calculate the density of the gas along the way to the camera. However, this was not done within the scope of this thesis as it is deemed to be too complicated and prone to introduce bias through assumptions.

This leaves a final point: how to get absolute concentration data from the PLIF measurement. In this work, the primary method has been to simply assume that if after profile division, a certain pixel has a value of one, that pixel has the concentration at which the profile image was recorded. Half the intensity would equal to half the concentration and so on. After this, correcting factors for quenching are applied as discussed in Section 5.3.4.

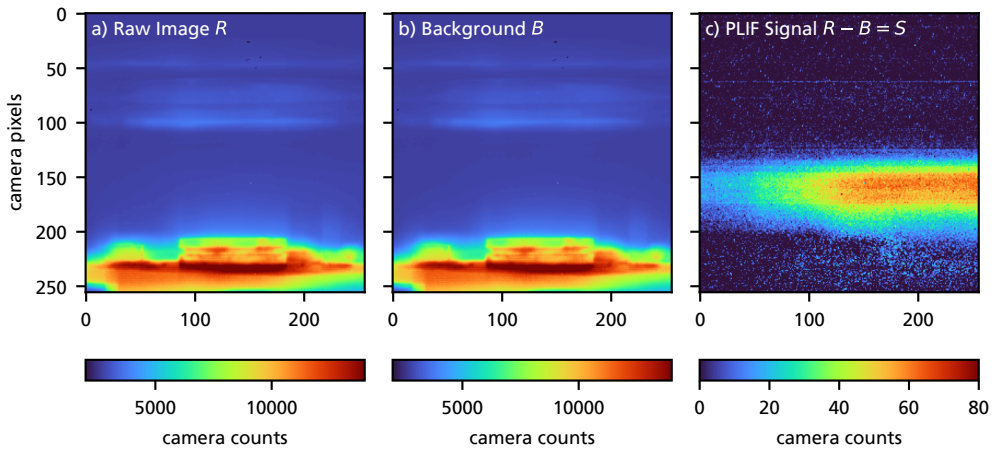

Figure 5.8: CO_2 PLIF Background Subtraction. Panel a) shows the image including the fluorescence data, while Panel b) shows a background image of the same situation taken without any laser light. The bright area at the bottom of the image is the hot sample holder, the rectangular shaped object just on top of this is the sample itself. The images look almost identical due to the very large background. Panel c) shows the data in Panel a) after the background has been subtracted. Note that the signal is only around 100 counts, while the background is several thousand.

5.3.4 Quenching

Although quenching is difficult to fully quantify, some attempts have been made as part of this thesis. First, some empirical CO_2 fluorescence measurements were performed where the partial pressure of CO, O_2, and a combination of the two was varied while the CO_2 concentration was kept constant at 6 mbar (4 %). The total pressure was 150 mbar and no sample was in the reactor. These measurements show that the O_2 concentration has little impact on the CO_2 signal, which is mainly affected by the CO concentration. However, in a reaction condition measurement in which the CO_2 fluorescence is measured, the CO concentration is not directly known. However, we have shown that the CO and CO_2 concentrations often appear to be inverted[1]. Thus, we can determine the probable CO concentration from the measured CO_2 concentration. Figure 5.10 shows the results of this measurement. Panel a) shows how the measured fluorescence signal depends on the CO concentration. By assuming that the CO concentration is the inverse of the CO_2 concentration, we can construct a function that relates the measured CO_2 concentration after background subtraction and profile division to the actual CO_2 concentration as shown in Panel b). This function can then be applied to the CO_2 fluorescence data shown in Panel c), resulting in the concentration map shown in Panel d). Finally, Panel e) shows the difference between the measured and actual concentrations. Note that where there is no CO_2, there is naturally no quenching as there is no signal to quench. Where there is a high

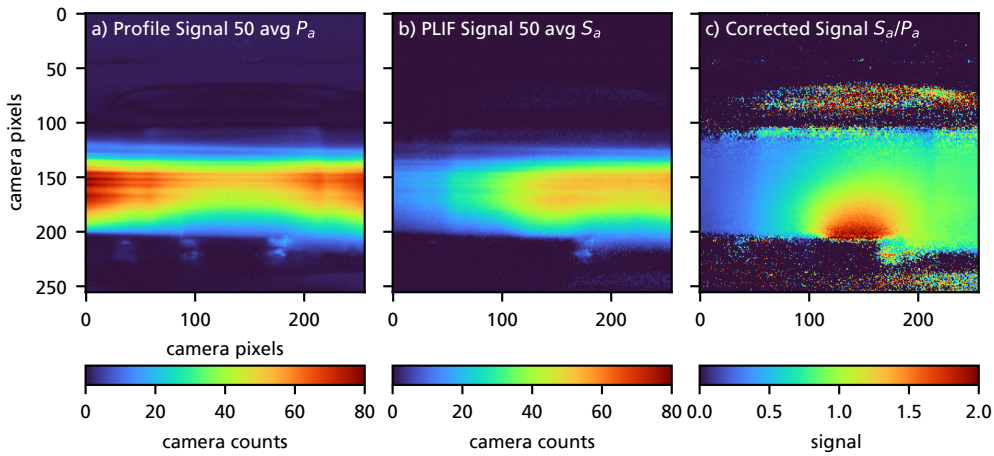

Figure 5.9: The Profile Division of the CO_2 PLIF images. Panel a) shows an average of 50 profile images acquired with the reactor filled with CO_2. Panel b) shows an average of the same number of images, but under reaction conditions where all CO_2 in the reactor originates from a catalytic reaction. By dividing these two, we can compensate for any inhomogeneities in the laser sheet intensity etc. The result is an image that clearly shows the gas cloud originating from the reaction shown in Panel c).

concentration of CO_2, close to the sample, there is little CO that can quench. The large differences are observed in the middle of the CO_2 cloud. Thus, we can conclude that while quenching by CO does affect the shape of the CO_2 cloud, it does not affect the measured CO_2 signal at the sample surface significantly.

We have also measured the decay of the CO_2 signal as a function of time by using a very short camera exposure time, and then scanning the delay of the camera trigger while keeping all other parameters constant. The results of this are shown in Figure 5.11. We can observe that the CO_2 signal first increases with the camera delay, but then, after 5–10 µs, it decreases exponentially. Two measurements are shown, one at 150 mbar total pressure where the CO_2 partial pressure us 6 mbar, and one at 900 mbar where the CO_2 total pressure is 36 mbar. By fitting an exponential function to the data points, we can determine that the decay in the 900 mbar case is 4 times faster than in the 150 mbar case. The conclusion of this is that quenching is indeed a major contributor to the decrease of the fluorescence signal over time. The red data points show the same measurement at reaction conditions, where all CO_2 in the reactor is produced by a catalytic reaction, which means that CO and O_2 are also present in the reactor. Here, we observe a large increase in the quenching, which confirms that quenching by CO is a major factor to consider, as discussed above.

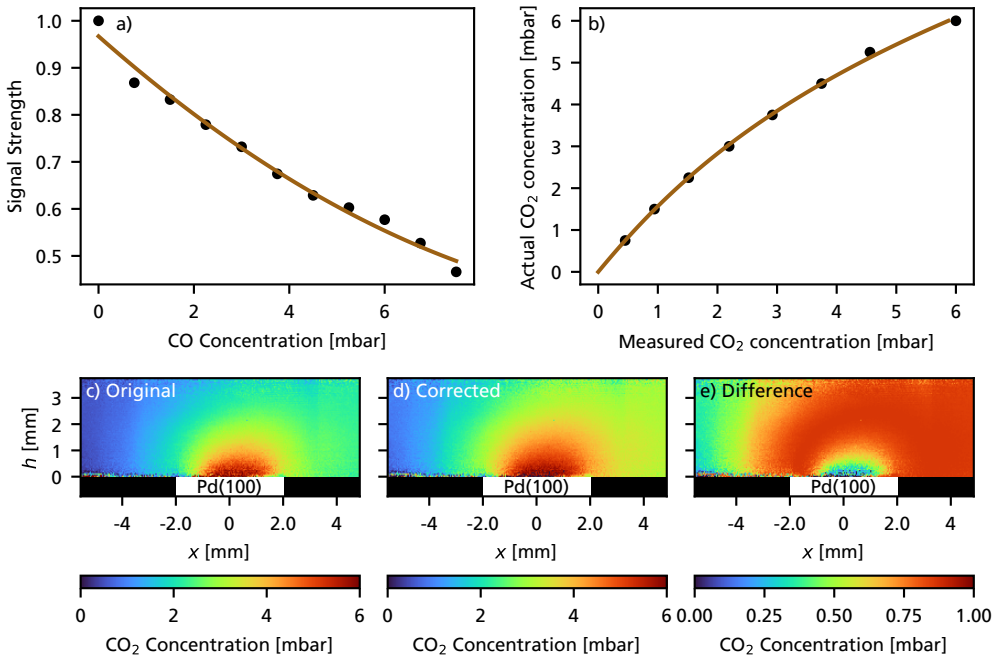

Figure 5.10: The results of empirical measurements to determine the quenching of the CO_2 signal by CO. Panel a) shows how much the signal decreases depending on the CO concentration while Panel b) shows how the measured CO_2 concentration relates to the actual CO_2 concentration, with the assumption that the CO and CO_2 concentrations are inverted throughout the reactor. Panels c) through e) show the effect of this applied to images of the CO_2 distribution over a working catalyst.

5.3.5 The Choice of Colour Map

On a last note, I would also like to discuss the choice of colour map when plotting images that show smooth gradients. Figure 5.12 shows the same data plotted with the *jet*, *turbo* and *viridis* colour maps. While this is of course subjective, the perception of the data can be significantly influenced by the choice of colour map. When using the classic *jet* colour map, as is the case in Panel a), cyan and yellow bands appear, which seem to separate the image into three zones, a "hot" zone where the concentration looks to be very high, as indicated by the presence of red colour, a medium zone between the yellow and cyan bands, and a low concentration zone where blue is dominant. The *turbo* colour map shown in Panel b) was developed to remedy this banding issue. However, it may still be perceived differently from linear colour maps such as *viridis* as shown in Panel c). In my personal opinion, the high concentration area close to the sample looks larger in b) than in c).

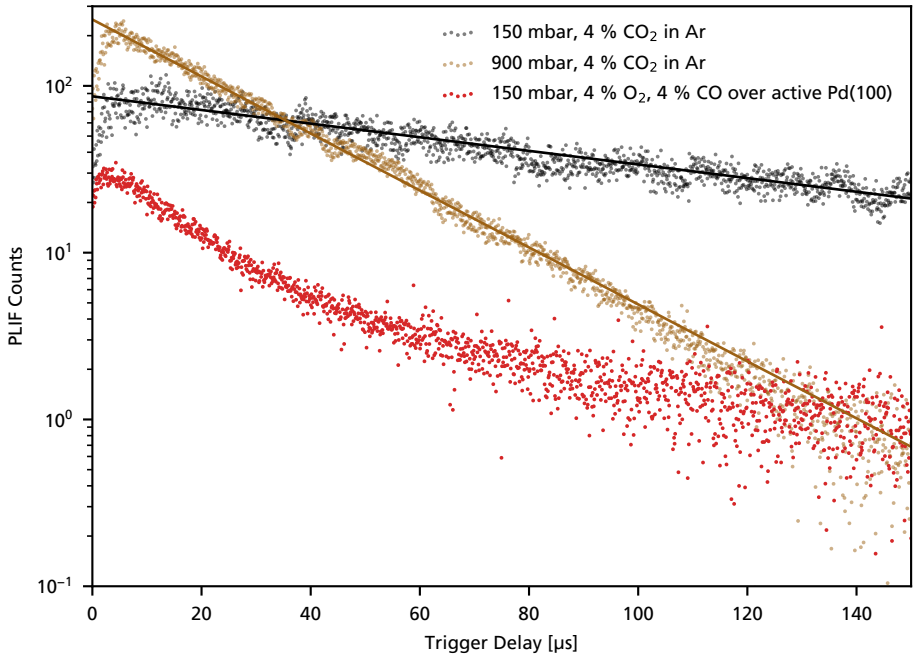

Figure 5.11: The CO_2 fluorescence as function of the camera trigger delay. Note that there is an increase of the signal within the first 10 μs, after which the signals decrease exponentially. The fluorescence at 900 mbar decays four times faster than that at 150 mbar, suggesting that the quenching is a major factor in the overall decay of the signal. The red data points show the decay of the signal at reaction conditions, when O_2 and CO are also present. This data seems to exhibit a combination of several exponential decay rates.

5.3.6 This Thesis

PLIF was used throughout this thesis to study the gas phase in *operando* catalysis experiments. Paper I treats the PLIF setup itself. In Papers II and III the PLIF setup is combined with 2D-SOR and HESXRD to study a catalyst during CO oxidation in oxygen-rich conditions. Paper V combines PLIF measurements with simulations of stagnation point flow measurements. Paper VI shows how PLIF can be used to measure gas temperatures. Finally, PLIF, and the thermal background is used in Paper IX together with 2D-SOR to visualise the ignition of a Pd(100) sample.

5.4 Temperature Measurements

Temperature is a central parameter in catalysis, since it controls the reaction rate of chemical reactions. Temperature data can also be used as an indicator of exothermic catalytic activ-

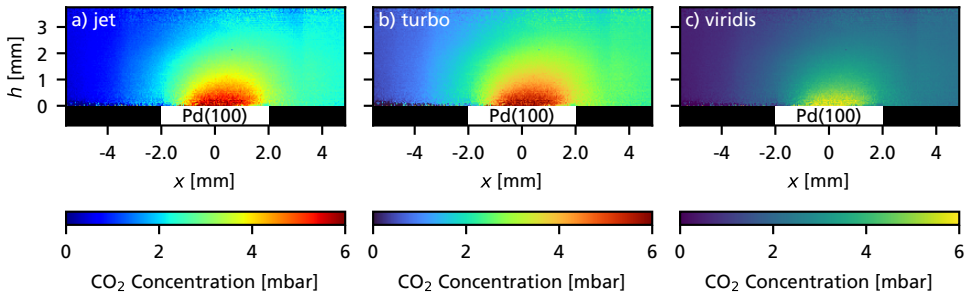

Figure 5.12: All three Panels show the same data. However, the choice of color map can change the perception of the PLIF data. When using *jet* as shown in Panel a), the data can appear split into a red zone, a yellow-cyan zone and a blue zone with sharp gradients between the zones. These gradient disappear when using the *turbo* colormap as shown in Panel b), however the image in b) may still be interpreted different from that in Panel c), where a linear color map, *viridis*, is used.

ity. The observation of the temperature of both the catalytic sample and the surrounding reactant and product gases as part of any catalysis experiment is thus of interest.

5.4.1 Sample Temperature

In this thesis work, temperature data were acquired in three ways. First, the sample temperature was monitored using a thermocouple attached to the sample holder. To calibrate the thermocouple temperature to the actual sample temperature, thermographic phosphors were used. There are phosphors that, when excited with a laser, emit light. The intensity of this light will decay exponentially with a temperature-dependent decay rate. More on this can be found in Paper **VI**.

The same IR camera that was used for the PLIF measurements can also be used to gain spatially resolved temperature data of the sample, also called thermography. This is especially useful for resolving the rapid temperature changes that occur at the sample ignition, as the IR camera can record instantaneous temperature data at up to 200 Hz. The temperature scale is then calibrated using the sample temperature reported by the thermocouple. Paper **IX** shows how this technique is used in combination with PLIF to investigate the kinetics involved in the catalytic ignition process.

5.4.2 Gas Temperature

As *operando* measurements are performed in a pressure range where the gas phase matters, it is important to know the temperature of the gas at different points in the reactor. Thus,

as part of this thesis work, three methods were investigated by which PLIF could also yield temperature information, without having to change the laser setup.

First, there is the ideal-gas law method. To use this method, two PLIF measurements are performed while the whole reactor is filled with CO_2. First, a measurement is made without any heating where the gas is assumed to be at room temperature, in this case around 20 °C. Then another measurement is made at a higher, unknown temperature. All the usual background subtraction is performed. From the ideal gas law $pV = nk_bT$, it is evident that if pressure and volume are kept constant, the number density is inversely proportional to the temperature. Thus, by dividing the two number densities, the temperature of the gas in the "hot" measurement can be determined. Correction factors have to be applied to correct for changes in population at higher temperatures, which can be found in the HITRAN database.

Second, there is the so-called calibration method, in which the gas just above the sample is assumed to have the same temperature as the sample. When the temperature of the sample is increased and thereby the temperature of the gas above the sample is increased, the number density at each temperature can be determined. This calibration curve can then be applied to the entire image, giving a spatially resolved temperature distribution.

Third, there is the spectral method. The key here is to use the fact that the shape of the CO_2 spectrum is quite wavelength dependent as shown in Figure 5.5. To use the spectral method, two measurements are performed, each at a different wavelength, but with otherwise equal parameters. The ratio of the intensities at each point in the two measurements can then be matched to a temperature. All three methods are elaborated in detail in Paper VI.

5.5 2D-Surface Optical Reflectance Microscopy 2D-SOR

2D-Surface Optical Reflectance is a technique by which the surface to be studied is illuminated at normal incidence with 660 nm LED light. The reflected light is then imaged by an sCMOS camera (Andor Zyla) through a microscope, resulting in a 2D image of the sample surface reflectivity. The use of the technique to study CO oxidation on Pd is rather new, and was further developed in this thesis[11, 12]. The experimental setup primarily used in this work is shown in Figure 5.13. The spatial resolution of the measurement is determined by the microscope magnification, while the temporal resolution is determined by the exposure time of the camera. The data acquisition rate is determined primarily by the read-out time of the camera sensor. In this work, the maximum rate at which images were acquired was 200 Hz, but much higher rates are possible if one uses a real high-speed camera. Since the signal strength is very high and primarily limited by the intensity of the LED, an 1:100 reflective beam splitter (also referred to as OD 1.3) can be used easily

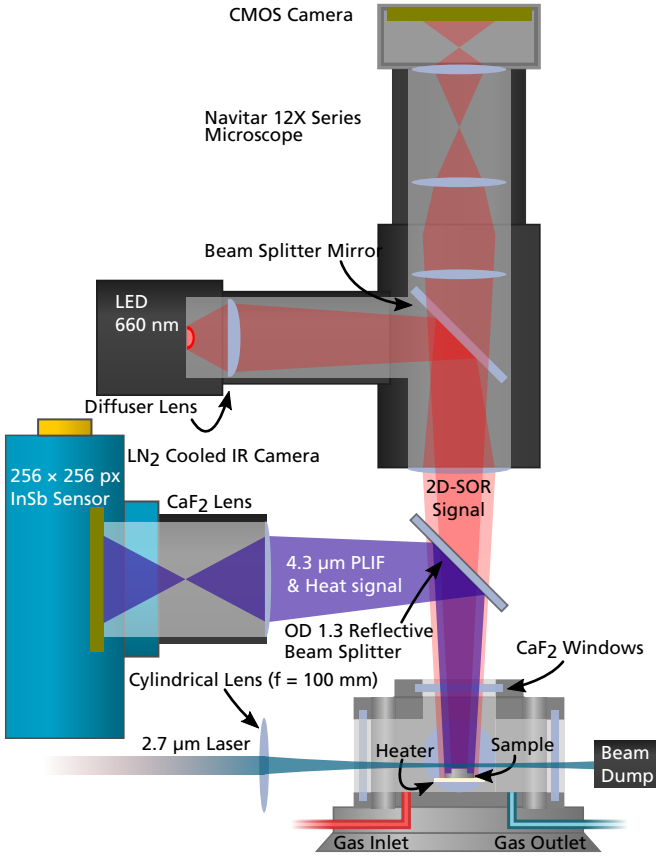

Figure 5.13: The 2D-SOR setup combined with PLIF set up to measure the reflectance of the sample and the CO_2 concentration in the gas near the sample from above. A red 660 nm LED is used to illuminate the sample. The reflection is then imaged through a microscope. To simultaneously obtain PLIF data, a reflective OD 1.3 filter is placed in the path of the reflected light which reflects the majority of the light into the IR camera, as the PLIF signal is much weaker than the 2D-SOR signal.

combine the PLIF, thermography and 2D-SOR techniques. In this case, the majority of the signal is used for PLIF. No filters are needed to distinguish the signals since the cameras are only sensitive in their respective wavelength ranges, which do not overlap.

5.5.1 Theory

In an attempt to investigate how the reflectivity of the surface depends on the thickness of an oxide layer, we can look at the Fresnel equations describing the reflection and transmission of light at a boundary. We begin by approximating the incident beam as plane waves with an electric field E. The polarisation of the light is not important since all light is polarised

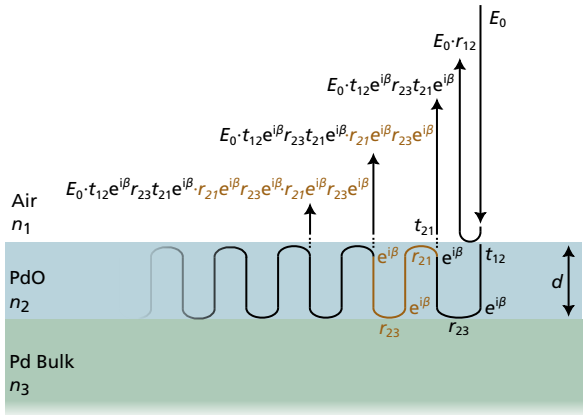

Figure 5.14: The light impinging on the oxide covered surface will reflect both off the oxide layer, the metal below the oxide, and also between the oxide and metal surfaces. Each time, the intensity is changed according to the Fresnel equation. Each ray leaving the surface results in another term. The terms all combine as shown in eq. (5.2)

parallel to the surface at normal incidence. We express the wave as

$$E = E_0 e^{i(kx-\omega t)},$$

where E_0 is the amplitude, $k = 2\pi/\lambda$ is the wavenumber and ω is the angular frequency of the wave. As the wave encounters a change in the refractive index at a boundary, the reflected and transmitted amplitudes E_r and E_t are given by the Fresnel equations[47]

$$E_r = \left|\frac{N_1 - N_2}{N_1 + N_2}\right| E_0, \quad E_t = \left|\frac{2N_1}{N_1 + N_2}\right| E_0,$$

where N_1 and N_2 are the refractive indices of the medium before and after the boundary. These refractive indices can be (and in this case are) complex in the form $N_i = n_i + i\alpha_i$, where the complex part is the damping of the wave in the medium and the real part is the usual refractive index that determines the speed $v = \omega/k = c/n$ of the wave in the medium. The quick explanation as to why this makes sense is to write the wave vector k in terms of N:

$$k = \frac{N\omega}{c} = \frac{n\omega + i\alpha\omega}{c}$$

Substituting this into the k in the plane wave equation above gives

$$E = E_0 e^{i\left(\frac{n\omega + i\alpha\omega}{c}x - \omega t\right)} = E_0 e^{i\left(\frac{n\omega}{c}x - \omega t\right)} \cdot e^{i\left(\frac{i\alpha\omega}{c}x\right)} = E_0 e^{i(kx-\omega t)} \cdot e^{-\frac{\alpha\omega}{c}x}.$$

So we get back the original plane wave together with a dampening factor, which corresponds to the normal Beer-Lambert law.

Back to the Fresnel equation. To simplify things a bit, we define r_{12} and t_{12} as the complex factors that determine how much of E_0 is reflected or transmitted when going from a medium with refractive index N_1 to another with refractive index N_2.

$$r_{12} = \frac{N_1 - N_2}{N_1 + N_2} = -r_{21}, \quad t_{12} = \frac{2N_1}{N_1 + N_2} = 1 + r_{12} = 1 - r_{21}. \tag{5.1}$$

This equation is for two layers. If we have an oxide film on a surface, we have three layers: air, oxide, and bulk metal. This means that things get more complicated. As the wave hits the oxide layer, the fraction r_{12} of the amplitude is reflected, while t_{12} is transmitted.

The part of the wave, which is transmitted by the first air-oxide boundary, continues into the oxide and has another chance to reflect off the second oxide-metal boundary. As the wave passes through the oxide with thickness d, it also picks up a factor $e^{iN_2 d/\lambda} = e^{i\beta}$, which accounts for both the phase difference picked up by travelling through the oxide and the attenuation by the oxide. This will happen twice every bounce, since the wave travels back and forth through the oxide. Each time the wave comes out of the oxide, it interferes with those that have already come out, resulting in a new term. This is repeated infinitely. Finally, the sum of all terms, each of which describes a complex amplitude, should be the total reflectance in the three layers r_{123}. The absolute square of that amplitude is the reflected intensity. We get

$$\begin{aligned} r_{123} = r_{12} & \\ & + t_{12} e^{i2\beta} r_{23} t_{21} \\ & + t_{12} r_{23} e^{i2\beta} t_{21} \cdot r_{21} r_{23} e^{i2\beta} \\ & + t_{12} r_{23} e^{i2\beta} t_{21} \cdot r_{21} r_{23} e^{i2\beta} \cdot r_{21} r_{23} e^{i\beta} \\ & + t_{12} r_{23} e^{i2\beta} t_{21} \cdot \left[r_{21} r_{23} e^{i2\beta} \right]^3 \\ & + \ldots \\ & + t_{12} r_{23} e^{i2\beta} t_{21} \cdot \left[r_{21} r_{23} e^{i2\beta} \right]^n , \end{aligned}$$

where the nth term corresponds to the nth reflected wave leaving the oxide. This can be rewritten as

$$\begin{aligned} r_{123} &= r_{12} + t_{12} r_{23} e^{i2\beta} t_{21} \left(1 + r_{21} r_{23} e^{i2\beta} + \left[r_{21} r_{23} e^{i2\beta} \right]^2 + \ldots + \left[r_{21} r_{23} e^{i2\beta} \right]^n \right) \\ &= r_{12} + t_{12} r_{23} e^{i2\beta} t_{21} \sum_{n=0}^{\infty} \left[r_{21} r_{23} e^{i2\beta} \right]^n = r_{12} + \frac{t_{12} r_{23} e^{i2\beta} t_{21}}{1 - r_{21} r_{23} e^{i2\beta}} \end{aligned}$$

Here, the sum is expanded in the last step. From (5.1) we get $t_{12} t_{21} = (1 + r_{12})(1 - r_{12}) = 1 - r_{12}^2$. Using this together with the fact that $r_{21} = -r_{12}$, and by putting all terms on a

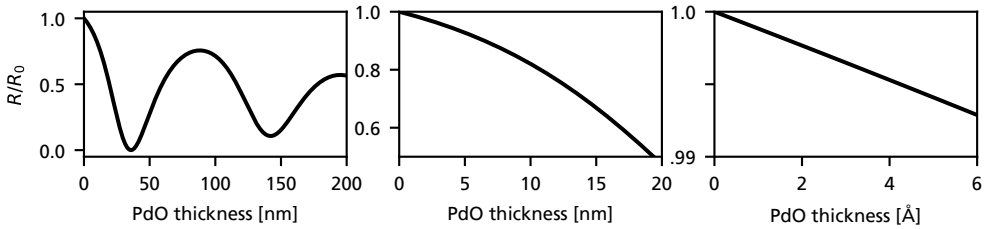

Figure 5.15: The reflected intensity for 660 nm light at normal incidence as function of the PdO film thickness. All panels show the same data, but with different resolution on the thickness axis.

common denominator, we get[48, 49]

$$r_{123} = \frac{r_{12}\left(1 + r_{12}r_{23}e^{2i\beta}\right) + \left(1 - r_{12}^2\right) r_{23}e^{2i\beta}}{1 + r_{12}r_{23}e^{2i\beta}} = \frac{r_{12} + r_{23}e^{2i\beta}}{1 + r_{12}r_{23}e^{2i\beta}}, \tag{5.2}$$

where $\beta = N_2 d/\lambda$. For 660 nm light, bulk PdO has a refractive index of $N_2 = 3.09 + 0.31i$[50], and metal Pd has a refractive index of $N_3 = 1.8 + 4.42i$[51]. Using these values in (5.2), and evaluating the total intensity $I_R = |E_0 \cdot r_{123}|^2$ produces the graphs shown in Figure 5.15. We conclude that *if* we assume that even very thin PdO has optical properties similar to those of bulk PdO, and *if* the surface stays smooth as is the case for thin surface oxides such as the $\sqrt{5}$-oxide, then we can use the reflected light to determine the oxide thickness. However any roughening caused by oxide formation is also expected to decrease the reflectivity.

5.5.2 Data Evaluation

In principle, the evaluation of the SOR image data is very simple. Once the images have been acquired, several images in which the sample is considered to be reduced, and thus the most shiny, are taken as reference images R_0. Then all other images are divided by the mean of these reference images, resulting in images in which the value of each pixel corresponds to the relative intensity R/R_0.

However, there are some caveats. First, there is a temperature dependence on the reflectance, whereby the reflectance of the sample changes if it is just heated in a mixture of CO and Ar with no oxide forming. This is attributed to a temperature dependence on the refractive indices involved. Figure 5.16 shows this effect. By fitting a linear function to the dependency, this effect can be corrected for in the data processing step.

The second caveat is that as the sample is heated, thermal expansion in the sample holder and reactor, as well as in the sample, causes the sample surface to shift slightly, around

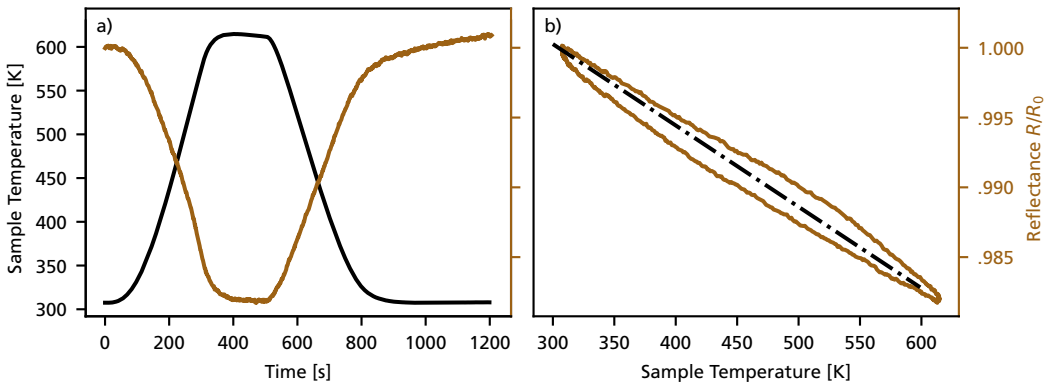

Figure 5.16: The reflectivity of the surface is rather linearly dependent on the surface temperature. Panel a) shows the results from a measurement whereby the temperature of a Pd sample is increased from 300 K to 600 K and then decreased back to 300 K. In Panel b), the reflectivity is plotted as function of the sample temperature, with a linear trend added. The slight hysteresis effect is attributed to a delay between the temperature of the sample surface and that at the the thermocouple attachment point.

10 µm, as well as raise slightly. This is not an issue when using a zoom where the whole sample is in frame. However, when zooming in, which is necessary for the polycrystalline samples that have grains on the tens of micrometre scale, this shift becomes very noticeable and results in both a loss of focus and a shift of the image, which renders per-pixel division problematic. The solution to these issues is to correct for this in post-processing, using motion tracking software to track imperfections in the surface and then compensating for the shift. The focus issue is alleviated by only ramping the temperature around the range of interest, after the focus is put in the middle of the temperature range to ensure acceptable focus throughout the measurement.

Third, there is the issue that has already been mentioned, that it is impossible to tell surface roughness apart from the formation of an oxide layer. In fact, any effect not directly related to the formation of an oxide is difficult to take into account. Some calculations have been made and it does in fact seem that roughness decreases reflectivity to a level similar to that of the oxide layer[12]. Due to this, only the papers in which 2D-SOR is used in combination with other techniques, such as Paper IV, make direct claims about the oxide thickness. However, it should be noted that, in all cases, the oxidised surface can be restored to the original reflectivity by reducing it in CO.

5.5.3 Conclusions

In summary, I think that 2D-SOR is an amazing technique, mainly due to its simplicity and low cost. However, one of its main strengths shows itself first when 2D-SOR is combined

with other techniques. When doing so, features in the 2D-SOR data that without context would simply be a "random dip in intensity", can be correlated to the formation of, for example, the $\sqrt{5}$-surface oxide. The combination of 2D-SOR with HESXRD and PLIF is discussed in Papers III and IX. 2D-SOR has also proven to be extraordinarily useful for studying polycrystalline samples, as shown in Paper VIII and in the experimental highlights section in Chapter 6.

5.6 Other Techniques Combined with 2D-SOR or PLIF

5.6.1 High-Energy Surface X-Ray Diffraction HESXRD

High-Energy Surface X-ray Diffraction (HESXRD) is a photon-in photon-out technique used to determine surface structures. As X-rays impinge onto the sample, each atom scatters the X-rays, resulting in a new spherical wave originating at that atom. The interference pattern of all of these waves is imaged by a large 2D detector. In order to make the technique surface sensitive, the geometry of the experiment is setup such that the X-rays impinge on the surface at a very shallow angle, resulting in total internal reflection. In this way, the bulk penetration of the X-rays into the bulk is significantly reduced resulting in a substantial surface contribution to the diffraction signal. By using a synchrotron as light source, a high beam intensity can be achieved which results in a strong diffration pattern that allows for a repetition rate of up to 10 Hz. In this thesis, I have combined HESXRD with PLIF and 2D-SOR, where HESXRD has been used to detect which oxide structures are formed on the surface as demonstrated in Papers III and II. For more information on the technique, see references 7 and 52.

5.6.2 Electron Backscatter Diffraction EBSD

Electron Backscatter Diffraction (EBSD) is a technique by which electron diffraction patterns from crystalline structures are captured and analysed to determine properties of the crystal lattice. The technique was first commercially availble in the 1990s. To perform a measurement, the sample is placed in a scanning electron microscope (SEM), and rotated so that there is a 70° angle between the electron beam and the sample. A fluorescent screen is placed close to the sample to record the diffraction patterns, so-called Kikuchi line patterns, as the beam is scanned across the sample surface. From the diffraction patterns the crystal orientation can be calculated at each scanned point. In this thesis work, EBSD was used to characterise the surfaces of polycrystalline Pd samples by mapping the orientation of the metal grains at the surface as shown in Paper VIII. Figures 3.3 and 3.4 show orientation mappings of polycrystalline samples performed using EBSD. Combining EBSD with other

techniques in an *in situ* measurement is challenging due to the closed nature of the commercial EBSD systems. However, unless the sample is heated to very high temperatures, one characterisation measurement per sample is sufficient, as the grains are not expected to change their orientation. For more information on the technique, see reference 53.

5.6.3 Polarisation Modulation Infrared Reflection Absorption Spectroscopy PMIRRAS

Polarisation Modulation Infrared Reflection Absorption Spectroscopy (PMIRRAS) is a technique to detect surface adsorbates. It works by shining broadband mid-IR light created by a filament onto the sample surface at a very shallow angle. Prior to impinging on the surface, the IR light is polarisation modulated at around 80 kHz. The adsorbates on the surface will interact differently with the different polarisations, as they are restricted in their degrees of freedom of movement due to their interaction with the surface. On the other hand, gas molecules have no such restrictions and can move freely in all directions, which means they interact equally to all polarisations. Thus, by comparing the adsorption of the different polarisations, the contribution by the surface can be extracted. The light reflected off the surface is collected by a point detector. If this light is spectrally resolved, for instance, by using a Fourier transform infrared spectrometer as light source, an adsorption spectrum of the surface adsorbates can be measured. For more details, see ref [54]. In this thesis, PMIRRAS was combined with 2D-SOR as shown in Paper VII.

5.7 Combining Techniques

This thesis work has focused primarily on combining two or more spatially resolved techniques. Usually, one of the techniques measures the gas phase, and the other monitors the surface. The spatially resolved techniques can also be combined with non-spatially resolved techniques. When combining multiple techniques, there are two types of challenges. First, there are the geometric challenges that arise when probing the sample with multiple techniques. There simply has to be enough space to place the equipment. Different techniques have different limitations in this respect. PLIF for instance requires optical access to the sample from three directions. Two of these must be facing each other to allow the laser to enter and exit the reactor, and the third must be perpendicular to the first two to image the fluorescence. 2D-SOR only needs one access from one direction, but this must be perpendicular to the sample surface. HESXRD needs access from two directions not blocked by anything else, and the whole reactor needs to rotate, the further the better. And I have not even mentioned the different materials that the enclosure must be made of for all this to work.

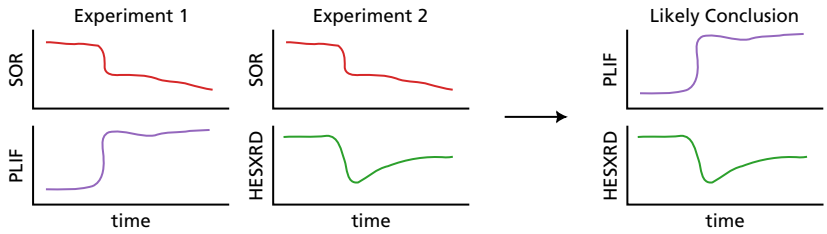

Figure 5.17: As long as one technique, in this case 2D-SOR, is used in multiple experiments, this can indirectly correlate other techniques, which may be challenging to otherwise combine.

Second, there are challenges in synchronising the signals from different techniques. This has been a challenge throughout this thesis work. Every camera or detector has its own software, sometimes even its own dedicated computer that must be used for compatibility reasons. Ensuring all detectors start the measurement simultaneously is crucial. Some manufacturers provide a software interface for their equipment, which can be used to integrate this into the control software used, but this also requires significant software development efforts. Another factor is that Ethernet, which is often used for communication between computers, offers very reliable communication but rather unreliable timings. The way detector software logs timestamps can also be a challenge. Some software stores a timestamp with every captured image. However, other software only stores the time at which the data file was created, which may or may not be when the data in the file was actually acquired.

Once the data have been collected, there are challenges related to data analysis. First, the data from the different detectors has to be loaded into the same software, to correlate them. This has resulted in a considerable amount of reverse engineering of file formats and the development of custom viewing software. Second, all of these data should be analysed, interpreted, and presented in a meaningful way, where the strengths of each technique are used to their full extent without creating plots that contain too much clutter.

However, the insights gained from a carefully executed multiple-technique experiment is without a doubt more than the sum of its parts. In this thesis, the gas in the reactor is usually analysed with both mass spectrometry and PLIF while the surface is usually monitored using 2D-SOR. Furthermore, 2D-SOR is a very convenient technique to combine with other techniques, as it requires access from one single direction and uses inexpensive equipment that is easy to transport.

The fact that 2D-SOR is so easy to transport and use also makes it a powerful "fingerprint" technique to indirectly compare other techniques as shown in Figure 5.17. For example, at the catalytic ignition of the Pd(100) surface, a small but sudden decrease can be seen, as discussed in Papers IV and IX. In the first of these papers, this dip has been correlated with the formation of a thin surface oxide as seen in HESXRD. We have also observed with PLIF

that the gas phase changes significantly as the dip occurs. Thus, we can assume that the change in gas coincides with a change in surface oxidation, which can then be investigated more to gain further certainty.

Chapter 6

Experimental Highlights

This chapter will treat some of the most beautiful results of this thesis work and take you on a journey from self-sustained oscillations to polycrystalline library samples. It will also be a story that showcases the usefulness and wide applicability of the 2D-SOR technique.

6.1 Reaction Oscillations during CO Oxidation

The tale begins with some beautiful measurements performed at DESY, where PLIF, 2D-SOR, and HESXRD were combined in a single measurement to study the oscillatory behaviour of the catalytic activity of a Pd(100) surface during CO oxidation. The experimental setup is explained in Paper III. It turns out that, under oxygen-rich conditions, the catalytic activity begins to oscillate and that these self-sustained oscillations go on for several hours. Figure 6.1 shows around 15 minutes of data where the catalyst exhibits such oscillations. The gas conditions were 50:1 O_2:CO with an oxygen partial pressure of 150 mbar and a CO partial pressure of 3 mbar. Ar was added for a total pressure of 240 mbar. Panel a) shows the product CO_2 concentration at the sample surface measured by PLIF, as well as the CO_2 and CO concentrations at the reactor outlet as measured by MS. Panel b) shows the 2D-SOR signal in an area of 1 by 1 mm in the centre of the 6 mm diameter sample. Here, the spatial resolution of the 2D-SOR technique was mainly used to verify that the entire sample behaved homogeneously, which it did to a large extent. Panel c) shows trends of a number of regions in the HESXRD diffraction images corresponding to the metal Pd(100) surface, PdO, and a metal Pd(111) surface. The sudden jerks in the data are due to height adjustment of the sample which was necessary as the sample temperature was not stable, resulting in thermal expansion. Finally, Panel d) shows the sample temperature as measured both with a thermocouple and using the PLIF background images.

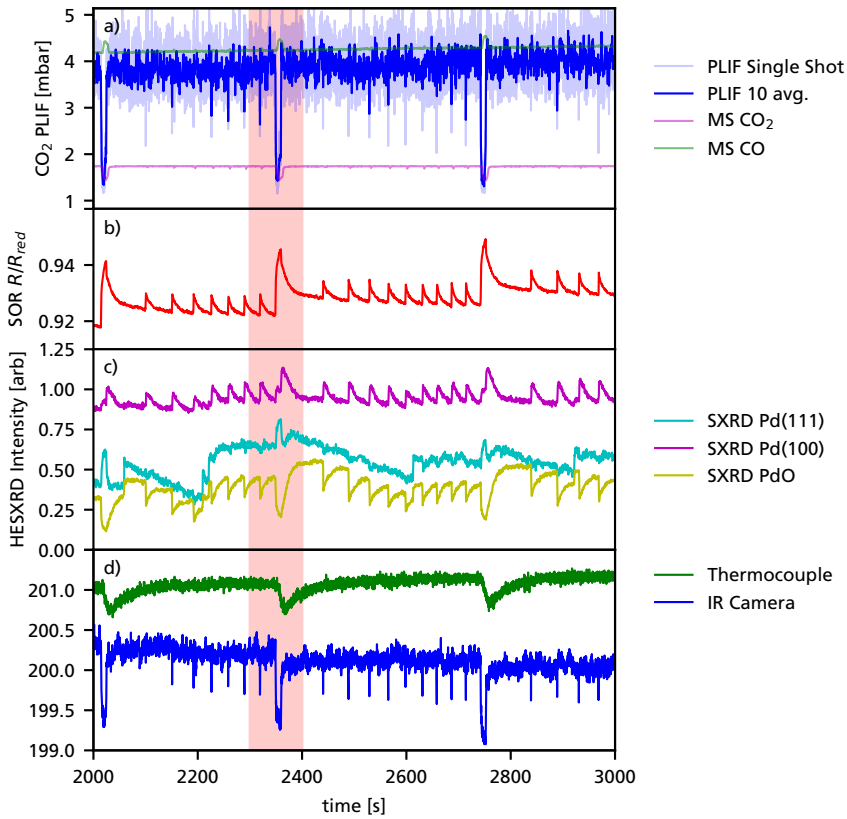

Figure 6.1: Data acquired during CO oxidation over a Pd(100) sample as the sample exhibits an oscillatory behaviour in its catalytic activity. Panel a) shows the gas phase data as measured with PLIF and MS. Panel b) shows the 2D-SOR reflectivity data and Panel c) shows the HESXRD trends which correspond to ROIs in the detector images. The trends are jerky due to sample readjustment as the sample and sample holder temperatures are not fully stabilised during the measurement. Panel d) shows the sample temperature as provided by a thermocouple attached to the sample holder as well as the thermography background images.

Approximately every 400 s, we observe a larger dip in the CO_2 production. These dips are preceded by a number of smaller dips. Figure 6.2 shows the data in the red area in detail, which contains one small and one large dip. The new pink line in Panel c) shows the inverse of the 2D-SOR signal in Panel b) for easy comparison. We observe that in the case of the small dip at around 2320 s, the dip is observed both in the CO_2 activity, as well as in the sample temperature, which makes sense since the reaction is exothermic. Furthermore, we observe that the PdO signal in the HESXRD data sharply decreases at the dip, coinciding with an increase in the metal signal, indicating a reduction of the oxide thickness. Within approximately 20 s, both signals return to their original value. The shape of the 2D-SOR signal follows this trend almost perfectly, indicating that 2D-SOR is a good

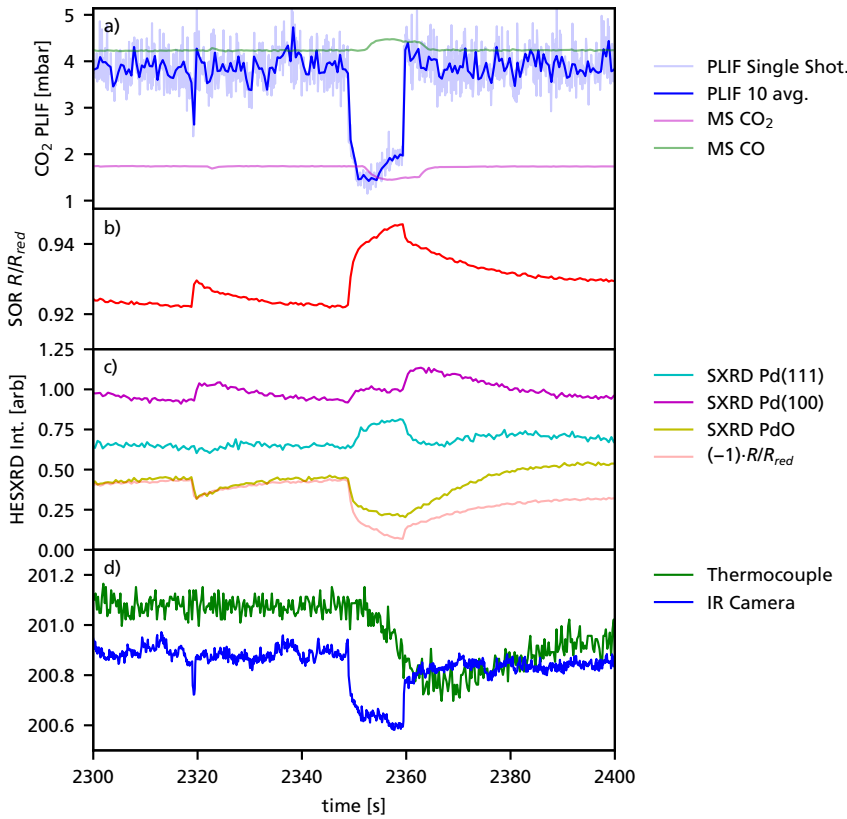

Figure 6.2: A magnification of the red area in Figure 6.1 showing two of the activity dips in the oscillations, a small and a large dip, in detail.

metric of surface oxidation under these conditions.

Moving on to the large dip at around 2350 s, we again observe a dip both in the CO_2 production and in the temperature data. This time, we see the dip not only in the IR-temperature data but also in the thermocouple, which has a much slower response as it is connected to the sample holder close to the sample. In the HESXRD data, we now observe two bumps in the metal Pd(100) data, the first of which coincides with a decrease in surface oxide. We also observe the emergence of a Pd(111) signal, which suggests the formation of Pd(111) islands together with the oxide, perhaps even on top of the oxide. The 2D-SOR signal initially follows the oxidation; however, it seems to decrease additionally, instead exhibiting a correlation with both the oxide formation and that of the presumed Pd(111) islands. This suggests that the change in reflectance caused by the Pd(111) results in an additional decrease of the 2D-SOR signal.

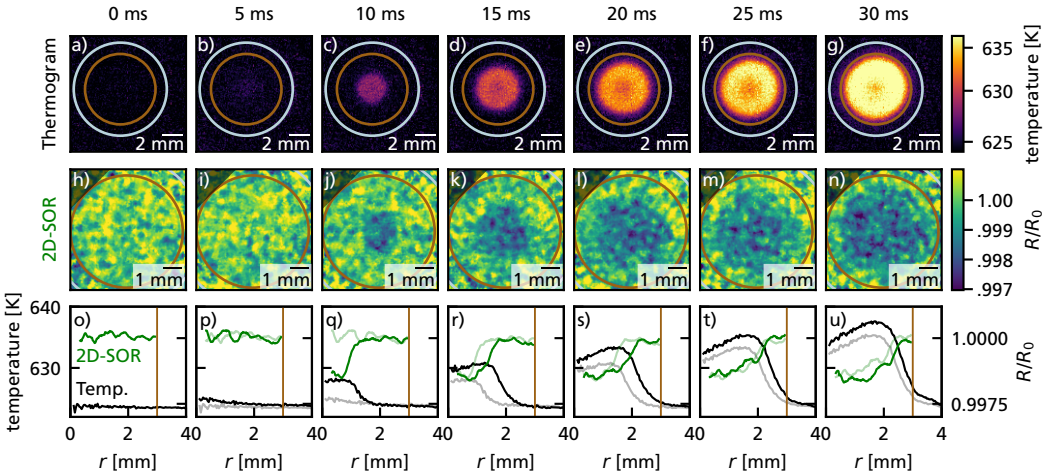

Figure 6.3: The catalytic ignition of a Pd(100) sample during CO oxidation. Panels a) – g) show the evolution of heat distribution on the sample during the iginition while Panels h) – n) show the evolution of the reflectivity as imaged with the 2D-SOR setup. Panels o) – u) show radial trends of both datasets.

6.2 Visualizing the Ignition of Pd(100) Single Crystal

This section will be a short summary of the beautiful results in Paper IX. In this paper, we have studied a Pd(100) sample during CO oxidation under oxygen-rich conditions. In the experiment, the sample temperature was slowly increased while PLIF and 2D-SOR measurements were performed from above, showing the sample surface. We also acquired background IR images at the highest rate possible with our camera, 200 Hz. In this way, we were able to follow the catalytic ignition itself. This occurs when the sample rapidly transitions from being CO covered and limited in its activity by the number of available sites to a highly active state where the activity is primarily limited by the diffusion of products and reactants.

Figure 6.3 shows this ignition phase with the reactor pressure at 900 mbar. We show that the sample suddenly ignites in the centre of the sample, forming a hotter area because the reaction is exothermic. The ignited, hotter, area then grows in size until it covers the entire sample. Simultaneously, the 2D-SOR data shows a dark area growing on the sample attributed to oxide formation. This area matches the ignited area, suggesting that an oxide forms quickly on the active parts of the sample.

The measurement was repeated at 150 mbar, and we show that the speed of the reaction wave matches the gas diffusion speed for both the 900 mbar and 150 mbar cases. We thus conclude that we see a gas-phase-driven ignition. As the surface adsorbates and the gas phase composition are coupled, changes in the gas phase affect the surface composition. In

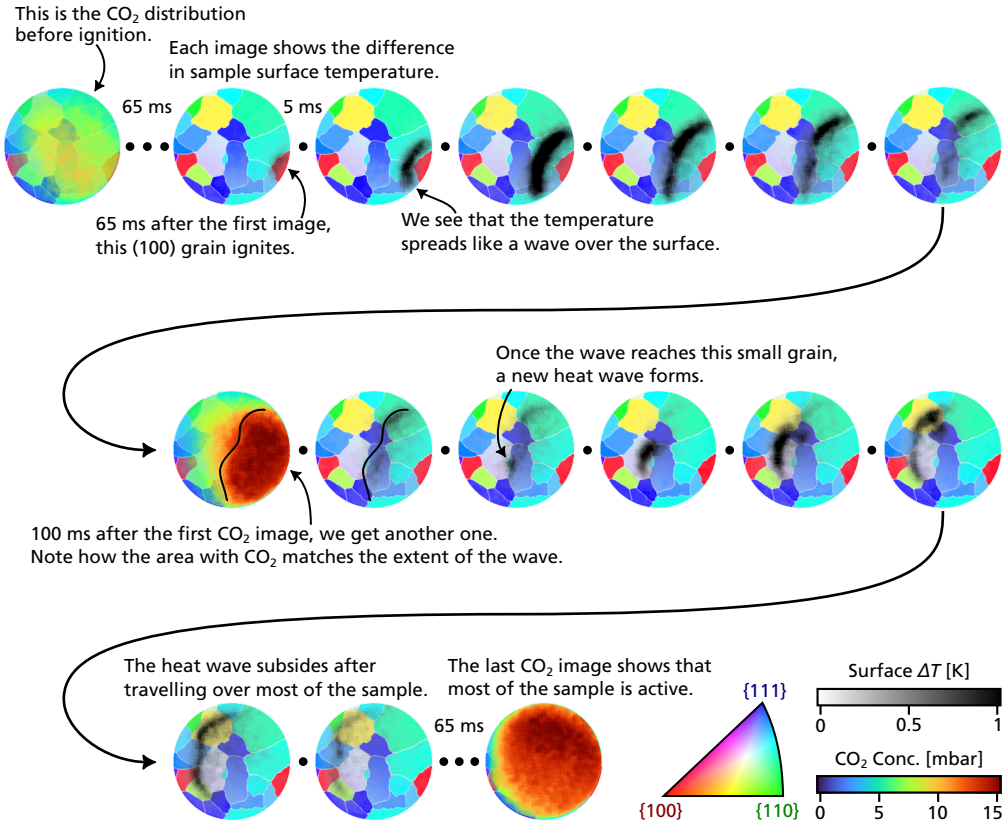

Figure 6.4: PLIF and Thermography images showing the ignition of a 7 mm diameter polycrystalline Pd sample. The background of the images shows the grain orientation as measured with EBSD. The rainbow color map images show the CO_2 concentration as measured with PLIF while the black color map images show the *difference* in temperature from the previous image.

this case, because we are under oxygen-rich gas conditions, ignition results in depletion of CO in that area. The CO-depleted gas cloud then diffuses over the sample surface, igniting more of the sample in a chain reaction. For more details on this, see Paper IX.

6.3 Polycrystal Ignition

We have also conducted similar measurements with the polycrystalline sample with large grains presented in Section 3.1.3, where the imaging capabilities of the 2D-SOR, PLIF, and IR thermography techniques show their full potential. We expected to be able to resolve the ignition of the individual grains, which should have been dependent on their intrinsic catalytic activity. Instead, we observe an effect similar to that of the single-crystal ignition. The ignition starts at one point on the sample and then spreads over the sample at the

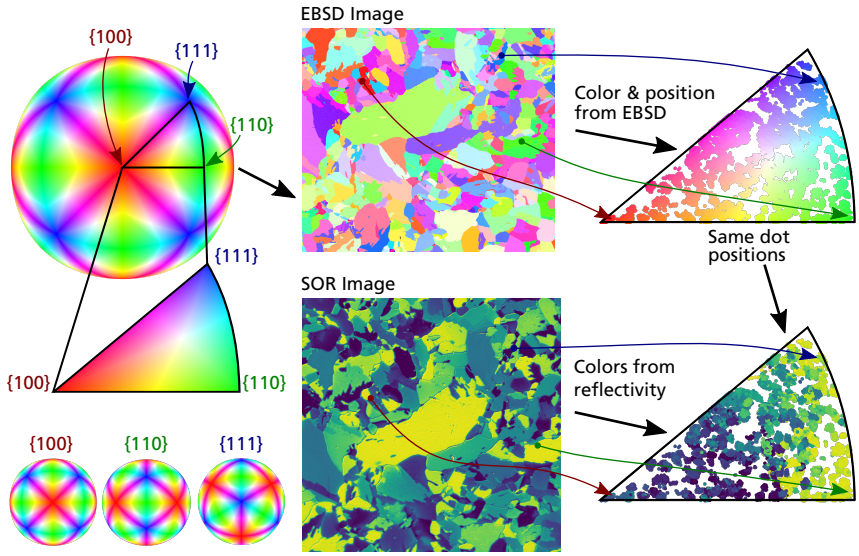

Figure 6.5: Visualisation of the 2D-SOR data in the stereographic triangle. To obtain the quasi-contious reflectivity map, first the orientation of each grain is determined with EBSD. Subsequently, the orientations are plotted in the stereographic triangle. Then the reflectivity of each grain can be plotted in the same triangle, at positions corresponding to the determined orientations.

speed of the gas diffusion, covering the entire sample within milliseconds. In contrast to the single-crystal case, the ignition front does not originate from the sample centre. The front also slows at some grain borders, indicating that the change in orientation brings with it a change in ignition temperature. This causes the ignition wave to briefly pause at some grain borders. The ignition quickly resumes once the CO-depleted gas reaches the next grain, or the temperature of the less active grain has been increased to the point where ignition occurs. We conclude that the grains on a polycrystalline surface do affect each other, which must be taken into consideration when polycrystals are used as surface orientation library samples.

6.4 Polycrystals with Small Grains

So what happens when the grains of the polycrystal are so small that any differences in gas phase composition are equalised very quickly due to diffusion? The polycrystalline sample with small grains presented in Section 3.1.3 contains hundreds of grains and we have mapped the grains in an ROI of approximately 1.5 mm² with EBSD. We then used 2D-SOR to study the oxidation of the sample during CO oxidation. Combining the 2D-SOR data together with the EBSD data in a sensible way was a challenge. In the end, we used the

same colour scale that was used in the 2D-SOR images to plot the reflectivity decrease of each grain in the position of the projection in the stereographic triangle corresponding to the surface orientation of that grain. This results in a quasi-continuous plot of reflectivity as a function of the surface orientation as illustrated in Figure 6.5. This way of plotting the data is, of course, not limited to 2D-SOR but could be implemented with any technique that can resolve a catalytically relevant property on a per-grain basis.

The experiment itself was quite straightforward; the sample was heated in oxygen-rich conditions (10:1 O_2:CO ratio at 150 mbar total pressure) while monitoring the sample surface using the 2D-SOR microscope. The gas composition was monitored using MS, as shown in Figure 6.6a). Panel a) also shows trends of the 2D-SOR signal for three of the grains denoted α, β and γ. Panels b) – d) show the 2D-SOR image of the sample in regions 1, 2, and 3 after dividing with an image of the sample in its reduced state. Although not much can be seen at the ignition — any ignition front would cross the whole imaged area in less than one frame — certain grains remain darker after the ignition. This is attributed to the formation of oxides. Panels e)–g) show the same data, but plotted in the stereographic triangle according to the orientation of the respective grain. We observe that at the ignition, primarily the grains in the (100) and (111) corners become darker, which is attributed to the formation of a thin surface oxide. As we continue to heat the sample, the reflectivity of many grains is reduced significantly, suggesting the formation of a thicker oxide. We see that the grains closer to the (100) orientation oxidise easier while those closer to (110) or (111) remain more reduced. Finally, in region 3, most grains except those very close to the (110) and (111) directions are covered with a thick oxide.

Another way to quantify the properties of the various surfaces exhibited by the grains is to use the concepts of the step density parameter (SDP) and the step edge parameter (SEP), which have been introduced by Winkler et al.[25]. The SDP gives an indication of how stepped the surface is compared to the (111) surface, while the SEP indicates how kinked the surface is. Figure 6.7 shows the oxide thickness calculated from the 2D-SOR image in region 2 (see Fig. 6.6) as a function of SEP and SDP. We observe a clear correlation between oxide thickness and SDP as shown in Panel a). Only the grains close to (110) coloured green deviate from the overall trend. Within the green grains, however, there is a similar trend. We observed no correlation between the SEP and the oxide thickness as shown in Panel b). This could be due to reconstruction of the kinked edges into longer straight segments under CO oxidation at higher pressures.

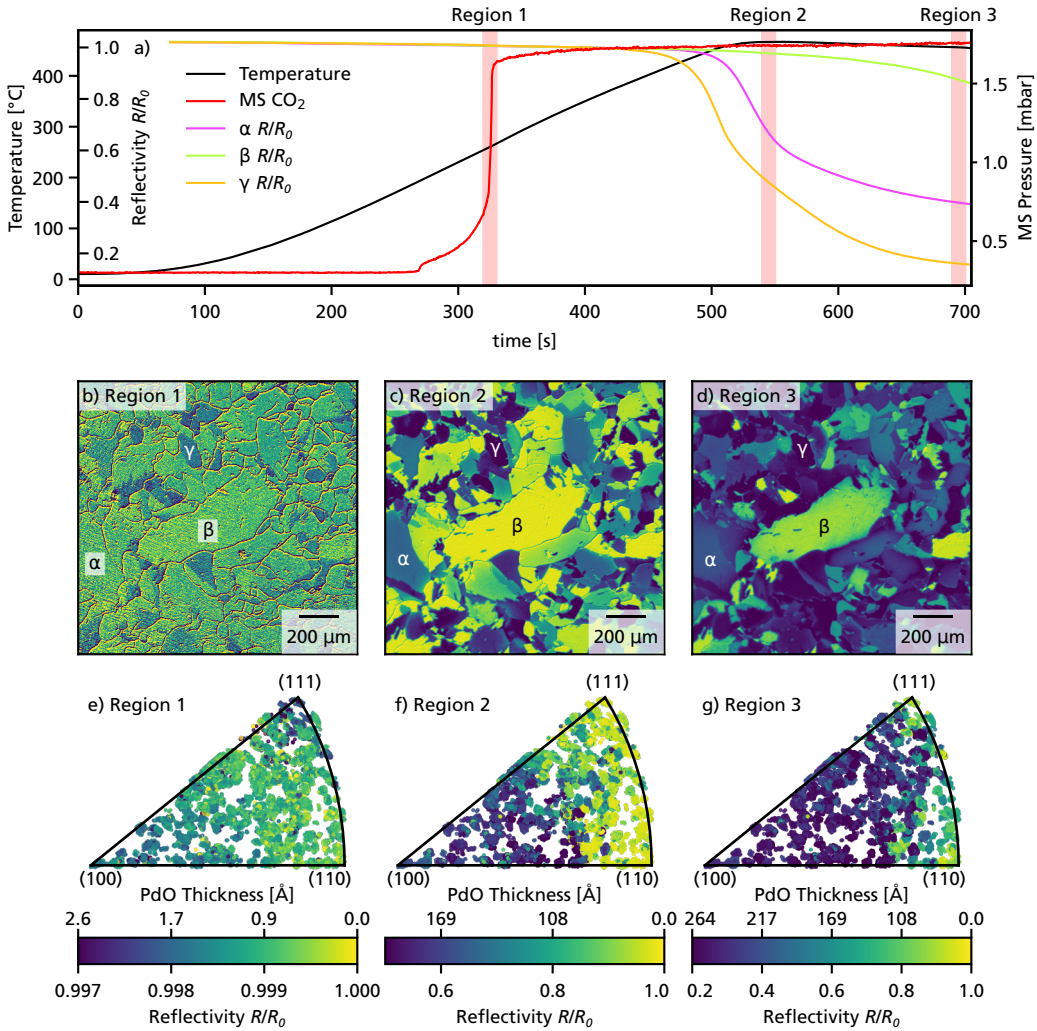

Figure 6.6: Results of the reflectivity study of the polycrystalline sample with small grains during CO oxidation. Panel a) shows the temperature ramp used in the experiments, the catalytic activity as indicated by the CO_2 MS trend and the reflectivity over time for three of the grains, α, β, and γ. Panels b) – d) show 2D-SOR images indicating the reflectivity loss when compared to a reduced sample in regions 1, 2, and 3 as indicated in a). Panels e) – g) show the same data plotted in the stereographic triangle according to the method presented in Figure 6.5.

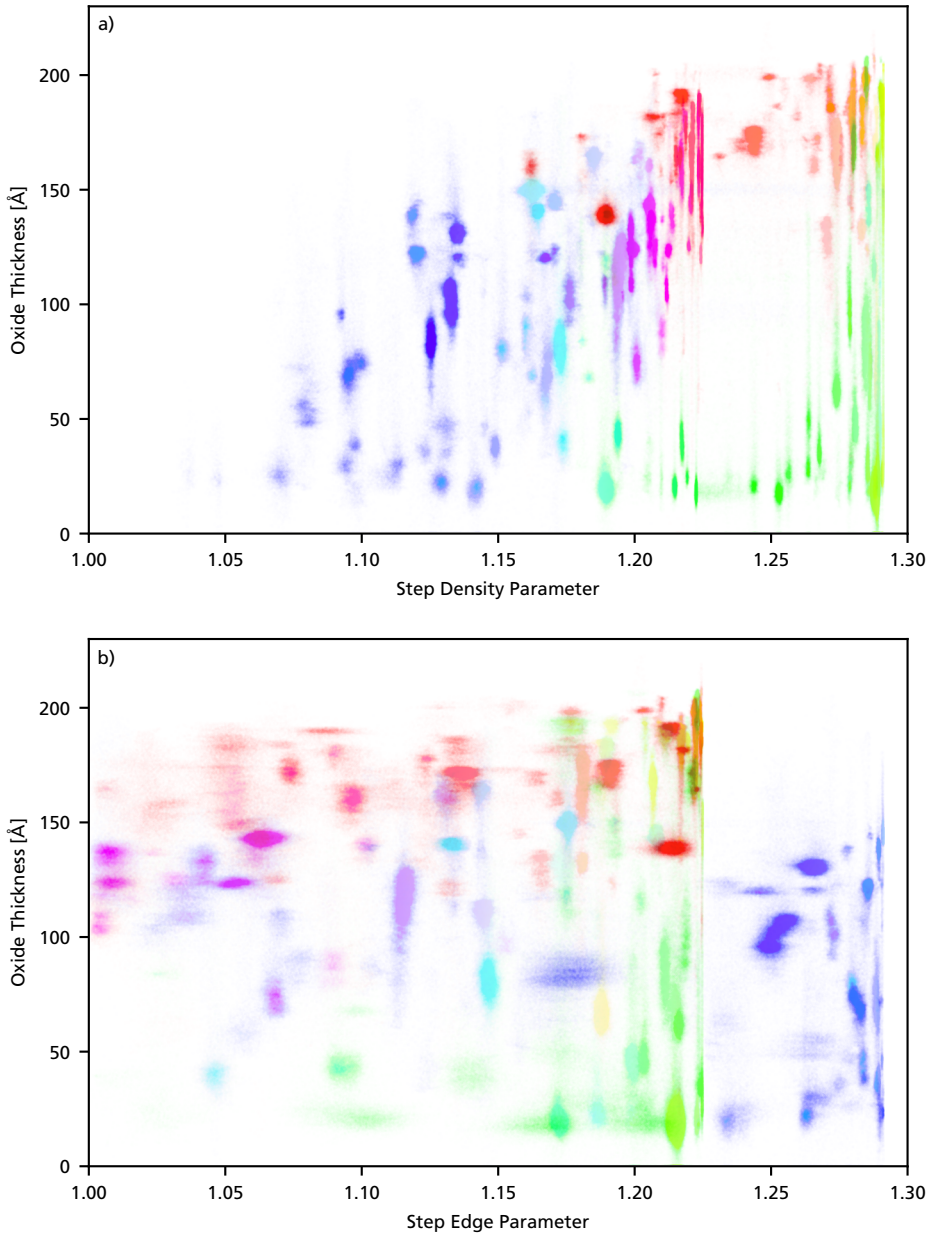

Figure 6.7: The oxide thickness of each grain as calculated from the 2D-SOR images as a function of the step density parameter (SDP) and the step edge parameter (SEP) of the corresponding surface. The colours indicate the orientation of the grain according to the color map in e.g. Figure 6.5. In panel a) we see a clear linear correlation between SDP and oxide thickness for all surface orientations except those close to the (110) surface. For the SEP in Panel b) no such correlation is observed.

Chapter 7

Outlook

In this chapter, I will first discuss possible developments of the two main stars of this work, the PLIF and 2D-SOR techniques. Then we will move on to possible future applications of the techniques, focusing on polycrystalline samples and the future of *operando* measurements.

First, with respect to PLIF, there are clear gains to be made by changing the laser and camera used. The laser system used in this work has a fixed 10 Hz pulse rate, which defines the data acquisition frequency. As the data presented in Section 6.3 and Paper **IX** shows, a frame rate of around 200 Hz is needed to visualise, for example, the catalytic ignition at atmospheric pressures. At lower pressures, even higher frame rates are needed. Thus, switching to a laser with a repetition rate of 200–1000 Hz would be very useful. In addition, the camera used for CO_2 PLIF has a resolution of only 256 by 256 px. Using a higher resolution camera would increase the spatial resolution of the technique as well as the resolution of the thermographic background. There are also more use cases of PLIF which have not been explored in this thesis. One feature of laser-based techniques, in general, is their ability to visualise very short-lived radicals, which has been used extensively in combustion diagnostics. However, this feature has to the my knowledge yet to be used in catalysis applications, where radicals may be present in the gas phase in the vicinity of the catalyst surface.

2D-SOR is also a technique where there are many possibilities for improvement. First, this thesis has focused on using a single wavelength of light to perform the measurements. Much more information could be gained by adding spectral resolution to the data, preferably without losing any spatial information. This could be achieved by performing a stroboscopic measurement in which multiple light sources are used that can be turned on or off. Spectral information would, for example, allow for an easier separation between oxide

thickness and roughening. In addition to this, the use of shorter wavelengths also allows us to resolve smaller details, since the resolution of the setup is diffraction-limited. Angle-resolved measurements are also a possibility that could be investigated further. Finally, the drift of the 2D-SOR image due to thermal expansion is also an issue, and further efforts could be made in post-processing to alleviate the issue.

It is also important not only to develop the individual techniques by themselves, but also to facilitate the combination of multiple techniques by considering such combinations already in the planning stage. 2D-SOR is an extremely useful augmenting technique as it requires optical access only from one direction. Although the technique does not provide direct quantitative information on the surface, it provides qualitative information with high spatial and temporal resolutions. Also, this qualitative information can be converted to quantitative information by "calibrating" the 2D-SOR signal with another technique such as the HESXRD in Section 6.1.

Moving on to the applications side, polycrystals have proven to be exceptionally useful in bridging the materials gap by providing data on many surfaces simultaneously, and are a perfect match with the spatially resolved techniques developed in this thesis. However, this thesis only scrapes the surface on what can be done with polycrystalline samples. For example, for easy comparison between datasets, most measurements presented in this thesis were performed under oxygen-rich conditions. As discussed in Paper IX, this causes an ignition feedback loop where the gas conditions caused be the ignition create a more favourable environment for further ignitions, causing the ignition to spread like a wave over the sample. If other gas conditions are chosen, this could probably be inhibited to the point where it could be possible to observe the ignition of individual grains. Thus, more measurements with polycrystals at different gas conditions should be considered. Also, there is one major issue with using EBSD to map the surface: EBSD is a bulk technique that does not take into account any potential surface reconstructions. The development of techniques that can measure the actual surface structure of each grain of the polycrystals would be extremely useful.

Finally, it should be said that as an increasing number of catalysis experiments are performed at higher pressures, there will be an increased need to understand the gas phase and how the coupling between the gas phase and the surface of the catalyst affects the progression of the chemical reaction in question. Thus, I believe that interest in combining spatially resolved gas-phase measurements with various surface sensitive techniques will only increase in the future.

References

1. Ertl, G., Knözinger, H., Weitkamp, J. *et al.* **Handbook of heterogeneous catalysis** (VCH Weinheim, 1997).
2. Ertl, G. **Reactions at Surfaces: From Atoms to Complexity (Nobel Lecture)**. *Angewandte Chemie International Edition* **47**, 3524–3535 (Apr. 2008).
3. Frenken, J. W. M. & Groot, I. **Operando research in heterogeneous catalysis** (Springer, 2017).
4. Lundgren, E., Zhang, C., Merte, L. R., Shipilin, M., Blomberg, S., Hejral, U., Zhou, J., Zetterberg, J. & Gustafson, J. **Novel in Situ Techniques for Studies of Model Catalysts**. *Accounts of Chemical Research* **50**, 2326–2333 (2017).
5. Starr, D. E., Liu, Z., Hävecker, M., Knop-Gericke, A. & Bluhm, H. **Investigation of solid/vapor interfaces using ambient pressure X-ray photoelectron spectroscopy**. *Chemical Society Reviews* **42**, 5833–5857 (June 2013).
6. Blomberg, Sara. **In situ structural studies and gas phase visualization of model catalysts at work**. PhD thesis (Lund University, 2017).
7. Gustafson, J., Shipilin, M., Zhang, C., Stierle, A., Hejral, U., Ruett, U., Gutowski, O., Carlsson, P.-A., Skoglundh, M. & Lundgren, E. **High-Energy Surface X-ray Diffraction for Fast Surface Structure Determination**. *Science* **343**, 758–761 (2014).
8. Hendriksen, B. L. M., Bobaru, S. C. & Frenken, J. W. M. **Looking at Heterogeneous Catalysis at Atmospheric Pressure Using Tunnel Vision**. *Topics in Catalysis* **36**, 43–54 (2005).
9. Zetterberg, J., Blomberg, S., Gustafson, J., Evertsson, J., Zhou, J., Adams, E. C., Carlsson, P.-A., Aldén, M., Lundgren, E., Alden, M., Lundgren, E., Aldén, M. & Lundgren, E. **Spatially and temporally resolved gas distributions around heterogeneous catalysts using infrared planar laser-induced fluorescence**. *Nature Communications* **6**, 7076 (2015).
10. Zhou, Jianfeng. ***Operando* Gas Imaging in Heterogeneous Catalysis**. PhD thesis (Lund University, 10 2018).
11. Onderwaater, W. G., Taranovskyy, A., Bremmer, G. M., Baarle, G. C. v., Frenken, J. W. M. & Groot, I. M. N. **From dull to shiny: A novel setup for reflectance difference analysis under catalytic conditions**. *Review of Scientific Instruments* **88**, 23704 (2017).
12. Onderwaater, W. G., Taranovskyy, A., van Baarle, G. C., Frenken, J. W. M. & Groot, I. M. N. **In Situ Optical Reflectance Difference Observations of CO Oxidation over Pd(100)**. *The Journal of Physical Chemistry C* **121**, 11407–11415 (2017).

13. Zhou, J., Blomberg, S., Gustafson, J., Lundgren, E. & Zetterberg, J. **Simultaneous Imaging of Gas Phase over and Surface Reflectance of a Pd(100) Single Crystal during CO Oxidation**. *The Journal of Physical Chemistry C* **121,** 23511–23519 (2017).

14. Freund, H.-J., Meijer, G., Scheffler, M., Schlögl, R. & Wolf, M. **CO Oxidation as a Prototypical Reaction for Heterogeneous Processes**. *Angewandte Chemie International Edition* **50,** 10064–10094 (2011).

15. Nolze, G. & Hielscher, R. **Orientations - Perfectly colored**. *Journal of Applied Crystallography* **49,** 1786–1802 (Oct. 2016).

16. Van Hove, M. A. & Somorjai, G. A. **A new microfacet notation for high-Miller-index surfaces of cubic materials with terrace, step and kink structures**. *Surface Science* **92,** 489–518 (Feb. 1980).

17. Zambelli, T., Wintterlin, J., Trost, J. & Ertl, G. **Identification of the "Active Sites" of a Surface-Catalyzed Reaction**. *Science* **273,** 1688–1690 (Sept. 1996).

18. Hendriksen, B. L., Ackermann, M. D., Van Rijn, R., Stoltz, D., Popa, I., Balmes, O., Resta, A., Wermeille, D., Felici, R., Ferrer, S. & Frenken, J. W. **The role of steps in surface catalysis and reaction oscillations**. *Nature Chemistry 2010 2:9* **2,** 730–734 (July 2010).

19. Hammer, B., Nielsen, O. H. & Nørskov, J. K. **Structure sensitivity in adsorption: CO interaction with stepped and reconstructed Pt surfaces**. *Catalysis Letters 1997 46:1* **46,** 31–35 (1997).

20. Smith, C., Hill, A. K. & Torrente-Murciano, L. **Current and future role of Haber–Bosch ammonia in a carbon-free energy landscape**. *Energy & Environmental Science* **13,** 331–344 (Feb. 2020).

21. Gurlo, A., Riedel, R., Gurlo, A. & Riedel, R. **In Situ and Operando Spectroscopy for Assessing Mechanisms of Gas Sensing**. *Angewandte Chemie International Edition* **46,** 3826–3848 (May 2007).

22. Grabow, L. C., Hvolbæk, B. & Nørskov, J. K. **Understanding trends in catalytic activity: The effect of adsorbate-adsorbate interactions for Co oxidation over transition metals**. *Topics in Catalysis* **53,** 298–310 (May 2010).

23. Garcia-Martinez, F., Schiller, F., Blomberg, S., Shipilin, M., Merte, L. R., Gustafson, J., Lundgren, E. & Ortega, J. E. **CO Chemisorption on Vicinal Rh(111) Surfaces Studied with a Curved Crystal**. *Journal of Physical Chemistry C* **124,** 9305–9313 (Apr. 2020).

24. Barroo, C., Wang, Z. J., Schlögl, R. & Willinger, M. G. **Imaging the dynamics of catalysed surface reactions by in situ scanning electron microscopy**. *Nature Catalysis* **3,** 30–39 (Jan. 2020).

25. Winkler, P., Zeininger, J., Suchorski, Y., Stöger-Pollach, M., Zeller, P., Amati, M., Gregoratti, L. & Rupprechter, G. **How the anisotropy of surface oxide formation influences the transient activity of a surface reaction**. *Nature Communications 2021 12:1* **12,** 1–8 (Jan. 2021).

26. Suchorski, Y. & Rupprechter, G. **Heterogeneous Surfaces as Structure and Particle Size Libraries of Model Catalysts**. *Catalysis Letters* **148,** 2947–2956 (Oct. 2018).

27. Orent, T. W. & Bader, S. D. **LEED and ELS study of the initial oxidation of Pd(100)**. *Surface Science* **115,** 323–334 (Mar. 1982).

28. Todorova, M., Lundgren, E., Blum, V., Mikkelsen, A., Gray, S., Gustafson, J., Borg, M., Rogal, J., Reuter, K., Andersen, J. N. & Scheffler, M. **The Pd(100)–(5×5)R27°-O surface oxide revisited**. *Surface Science* **541,** 101–112 (Sept. 2003).

29. Kostelník, P., Seriani, N., Kresse, G., Mikkelsen, A., Lundgren, E., Blum, V., Šikola, T., Varga, P. & Schmid, M. **The surface oxide: A LEED, DFT and STM study**. *Surface Science* **601,** 1574–1581 (2007).

30. Vincenti, W. G. & Kruger, C. H. **Introduction to Physical Gas Dynamics**, 11–15 (Krieger Publishing Company, Malabar, Florida, 1965).

31. Westerström, R., Wang, J. G., Ackermann, M. D., Gustafson, J., Resta, A., Mikkelsen, A., Andersen, J. N., Lundgren, E., Balmes, O., Torrelles, X., Frenken, J. W. & Hammer, B. **Structure and reactivity of a model catalyst alloy under realistic conditions**. *Journal of Physics: Condensed Matter* **20,** 184018 (Apr. 2008).

32. Ackermann, M. D., Pedersen, T. M., Hendriksen, B. L., Robach, O., Bobaru, S. C., Popa, I., Quiros, C., Kim, H., Hammer, B., Ferrer, S. & Frenken, J. W. **Structure and reactivity of surface oxides on Pt(110) during catalytic CO oxidation**. *Physical Review Letters* **95,** 255505 (Dec. 2005).

33. Hammer, B. & Norskov, J. K. **Why gold is the noblest of all the metals**. *Nature 1995 376:6537* **376,** 238–240 (July 1995).

34. Frank-Kameneckij, D. A. **Diffusion and heat transfer in chemical kinetics.** 2nd ed., 460–466 (Plenum Press, New York, 1969).

35. Ehsasi, M., Berdau, M., Rebitzki, T., Charlé, K. P., Christmann, K. & Block, J. H. **A reactive phase diagram of CO oxidation on Pd(110): Steady and oscillatory states**. *The Journal of Chemical Physics* **98,** 9177 (Aug. 1998).

36. Bowker, M., Jones, I. Z., Bennett, R. A., Esch, F., Baraldi, A., Lizzit, S. & Comelli, G. **Shedding light on catalytic ignition: coverage changes during CO oxidation on Pd(110)**. *Catalysis Letters 1998 51:3* **51,** 187–190 (1998).

37. Rijn, R. v., Ackermann, M. D., Balmes, O., Dufrane, T., Geluk, A., Gonzalez, H., Isern, H. *et al.* **Ultrahigh vacuum/high-pressure flow reactor for surface x-ray diffraction and grazing incidence small angle x-ray scattering studies close to conditions for industrial catalysis**. *Review of Scientific Instruments* **81,** 14101 (Jan. 2010).

38. Eckbreth, A. C. **Laser Diagnostics for Combustion Temperature and Species** 2nd ed. (CRC Press, London, Jan. 1996).

39. Huber, K. P. & Herzberg, G. **Molecular Spectra and Molecular Structure** (Springer US, 1979).

40. Kirby, B. J. & Hanson, R. K. **Linear excitation schemes for IR planar-induced fluorescence imaging of CO and CO2**. *Applied Optics* **41,** 1190–1201 (2002).

41. Zetterberg, J., Blomberg, S., Gustafson, J., Sun, Z. W., Li, Z. S., Lundgren, E., Alden, M. & Aldén, M. **An in situ set up for the detection of CO2 from catalytic CO oxidation by using planar laser-induced fluorescence**. *Review of Scientific Instruments* **83,** 53104 (2012).

42. Saleh, B. E. A. & Teich, M. C. **Fundamentals of Photonics** (John Wiley & Sons, Inc., New York, USA, Aug. 1991).

43. Kochanov, R. V., Gordon, I. E., Rothman, L. S., Wcisło, P., Hill, C. & Wilzewski, J. S. **HITRAN Application Programming Interface (HAPI): A comprehensive approach to working with spectroscopic data**. *Journal of Quantitative Spectroscopy and Radiative Transfer* **177,** 15–30 (July 2016).

44. Gordon, I. E., Rothman, L. S., Hargreaves, R. J., Hashemi, R., Karlovets, E. V., Skinner, F. M., Conway, E. K. *et al.* **The HITRAN2020 molecular spectroscopic database**. *Journal of Quantitative Spectroscopy and Radiative Transfer* **277,** 107949 (2022).

45. Aldén, M., Wallin, S. & Wendt, W. **Applications of two-photon absorption for detection of CO in combustion gases**. *Applied Physics B* **33,** 205–208 (1984).

46. Haumann, J., Seitzman, J. M. & Hanson, R. K. **Two-photon digital imaging of CO in combustion flows using planar laser-induced fluorescence**. *Optics Letters* **11,** 776–778 (1986).

47. Griffiths, D. J. **Introduction to Electrodynamics** 4th ed., 403–405 (Pearson, 2013).

48. McIntyre, J. D. & Aspnes, D. E. **Differential reflection spectroscopy of very thin surface films**. *Surface Science* **24,** 417–434 (Feb. 1971).

49. Heavens, O. S. **Optical properties of thin solid films**, 55–57 (Courier Corporation, 1991).

50. Nilsson, P. O. & Shivaraman, M. S. **Optical properties of PdO in the range of 0.5-5.4 eV**. *Journal of Physics C: Solid State Physics* **12,** 1423 (Apr. 1979).

51. Johnson, P. B. & Christy, R. W. **Optical constants of transition metals: Ti, V, Cr, Mn, Fe, Co, Ni, and Pd**. *Physical Review B* **9,** 5056 (June 1974).

52. Hejral, U. E. **Operando characterization of supported alloy nanoparticles during catalytic CO oxidation by surface sensitive x-ray diffraction**. PhD thesis (Universität Hamburg, 2015).

53. Stojakovic, D. **Electron backscatter diffraction in materials characterization**. *Processing and Application of Ceramics* **6** (Mar. 2012).

54. Hoffmann, F. M. **Infrared reflection-absorption spectroscopy of adsorbed molecules**. *Surface Science Reports* **3,** 107–192 (Jan. 1983).

Chapter 8

Scientific Publications

8.1 Author Contributions

Paper I: A Convenient Setup for Laser-Induced Fluorescence Imaging of both CO and CO_2 during Catalytic CO Oxidation

Zhou, J., Pfaff, S., Lundgren, E. & Zetterberg, J.

This paper discusses a semi-portable PLIF setup that can be used to detect CO and CO_2 in a catalysis reactor. Importantly, the setup is small enough to be hauled to synchrotrons in a truck in a reliable way. The paper also discusses the technical details of the approach.

I performed the experiments with J. Zhou, and we also performed the subsequent data analysis together. I also did the majority of work on the figures. J. Zhou wrote the manuscript.

Paper II: Combining Synchrotron Light with Laser Technology in Catalysis Research

Blomberg, S., Zetterberg, J., Gustafson, J., Zhou, J., Shipilin, M., Pfaff, S., Hejral, U., Carlsson, P.-A., Gutowski, O., Bertram, F. & Lundgren, E.

This paper discusses how the setup introduced in Paper I is used at DESY to perform HESXRD combined with PLIF. It shows how gas phase information can be correlated with spatial information and that the oxide appears shortly after the sample ignition.

I was involved in preparing the PLIF part of the beam time and performed the subsequent data analysis together with J. Zhou. I also contributed significantly to some of the figures. All the other authors were involved in the beam time.

Paper III: Combining High-Energy X-Ray Diffraction with Surface Optical Reflectance and Planar Laser Induced Fluorescence for *Operando* Catalyst Surface Characterization

Pfaff, S., Zhou, J., Hejral, U., Gustafson, J., Shipilin, M., Albertin, S., Blomberg, S., Gutowski, O., Dippel, A., Lundgren, E. & Zetterberg, J.

This paper concerns the technical details of the combination of 2D-SOR, the PLIF setup from Paper I and the HESXRD measurements presented in Paper II. We combine these techniques at a beam time at DESY, the results of which are reported in this paper.

I planned the PLIF and SOR parts of the experiment together with Zhou and Zetterberg and performed the data analysis. I prepared the manuscript and figures.

Paper IV: Surface Optical Reflectance combined with X-Ray Techniques during Gas-Surface Interactions

Albertin, S., Gustafson, J., Zhou, J., Pfaff, S., Shipilin, M., Blomberg, S., Merte, L. R., Gutowski, O., Dippel, A. C., Zetterberg, J., Lundgren, E. & Hejral, U.

In this paper, 2D-SOR and HESXRD are combined to see if it is possible to correlate changes in reflectivity with the formation of thin oxides. The paper confirms that oxide formation correlates with a change in 2D-SOR signal.

I planned the SOR part of the experiment together with Zhou and Zetterberg, participated in the beamtime, and performed parts of the data analysis.

Paper V: Combining Planar Laser-Induced Fluorescence with Stagnation Point Flows for Small Single-Crystal Model Catalysts: CO Oxidation on a Pd(100)

Zhou, J., Matera, S., Pfaff, S., Blomberg, S., Lundgren, E. & Zetterberg, J.

This paper explores the stagnation point flow configuration which is especially useful for simulation. The results of PLIF measurements are compared to simulations.

I participated in the experiments and the discussion of the paper. J. Zhou wrote the manuscript and made the figures.

Paper VI: Temperature Characterization of an *Operando* Flow Reactor for Heterogeneous Catalysis
Pfaff, S., Karlsson, H., Nada, F. A., Lundgren, E. & Zetterberg, J.

This paper concerns the temperature calibration of the reactor we use for our experiments. It treats both gas phase and sample temperatures.

I planned and performed the experiments concerning the gas phase temperature measurements and prepared the manuscript and figures.

Paper VII: Infrared Surface Spectroscopy and Surface Optical Reflectance for *Operando* Catalyst Surface Characterization
Rämisch, L., Gericke, S. M., Pfaff, S., Lundgren, E. & Zetterberg, J.

This paper treats the combination of 2D-SOR with PM-IRRAS. Technical aspects of the setup and the benefits and challenges of combining the techniques are discussed.

I took part in building the experimental setup and assisted with data analysis and acquisition. I also participated in discussions about the manuscript.

Paper VIII: *Operando* Reflectance Microscopy on Polycrystalline Surfaces in Thermal Catalysis, Electrocatalysis, and Corrosion
Pfaff, S., Larsson, A., Orlov, D., Harlow, G. S., Abbondanza, G., Linpé, W., Rämisch, L., Gericke, S. M., Zetterberg, J. & Lundgren, E.

In this paper we show that reflectance microscopy in combination with polycrystalline samples is a powerful technique, as the polycrystal can act as a collection of single-crystals. We resolve the response of multiple grains simultaneously in both thermal catalysis and electrochemistry.

I planned the experiments and prepared the manuscript together with A. Larsson. I focused on the thermal catalysis, including experiments, while Larsson focused on the electrochemistry.

Paper IX: Visualizing the Gas Diffusion Induced Ignition of a Catalytic Reaction
Pfaff, S., Rämisch, L., Gericke, S. M., Larsson, A., Lundgren, E. & Zetterberg, J.

This paper shows how thermography and PLIF can be combined to visualise the spatial evolution of the catalytic ignition process over a single-crystal sample. We argue that the ignition is driven by a coupling between the surface and gas phase.

I planned the experiments and performed the measurements together with A. Larsson. I performed the data analysis and wrote the manuscript. The other co-authors participated in the discussion of the results.

Printed by Media-Tryck, Lund 2022 NORDIC SWAN ECOLABEL 3041 0903

Division of Combustion Physics
Department of Physics

Lund Reports on Combustion Physics: LRCP-244
ISBN 978-91-8039-424-6
ISSN 1102-8718
ISRN LUTFD2/TFCP-244-SE